MCB
Journals.ASM.org

Amino Acid-Dependent mTORC1 Regulation by the Lysosomal Membrane Protein SLC38A9

Jennifer Jung, Heide Marika Genau, Christian Behrends

Institute of Biochemistry II, Goethe University School of Medicine, Frankfurt am Main, Germany

The serine/threonine kinase mTORC1 regulates cellular homeostasis in response to many cues, such as nutrient status and energy level. Amino acids induce mTORC1 activation on lysosomes via the small Rag GTPases and the Ragulator complex, thereby controlling protein translation and cell growth. Here, we identify the human 11-pass transmembrane protein SLC38A9 as a novel component of the Rag-Ragulator complex. SLC38A9 localizes with Rag-Ragulator complex components on lysosomes and associates with Rag GTPases in an amino acid-sensitive and nucleotide binding state-dependent manner. Depletion of SLC38A9 inhibits mTORC1 activity in the presence of amino acids and in response to amino acid replenishment following starvation. Conversely, SLC38A9 overexpression causes RHEB (Ras homolog enriched in brain) GTPase-dependent hyperactivation of mTORC1 and partly sustains mTORC1 activity upon amino acid deprivation. Intriguingly, during amino acid starvation mTOR is retained at the lysosome upon SLC38A9 depletion but fails to be activated. Together, the findings of our study reveal SLC38A9 as a Rag-Ragulator complex member transducing amino acid availability to mTORC1 activity.

The mechanistic target of rapamycin complex 1 (mTORC1) regulates cell growth and metabolism; therefore, its activity often is altered in cancer (1). mTORC1 comprises several subunits, including the serine/threonine kinase mTOR, regulatory-associated protein of mTOR (RPTOR), mammalian lethal with SEC13 protein 8 (MLST8), AKT1 substrate 1 (AKT1S1), and DEP domain containing mTOR-interacting protein (DEPTOR) (2, 3). The mTORC1 complex serves as a platform to integrate upstream signals, such as the nutritional state, growth factors, and energy level. Some of these signals, for example, insulin stimulation or low energy levels, are converged by phosphorylation of the tuberous sclerosis complex (TSC), as reviewed in reference 4. The TSC is composed of the proteins TSC1, TSC2, and TBC1D7 and acts as a GTPase-activating protein (GAP) for the small GTPase RHEB (Ras homolog enriched in brain), stimulating the transition from its active GTP-bound to its inactive GDP-bound state (5–7). RHEB is anchored to endomembranes, especially to lysosomes, via its prenylated C-terminal CAAX box motif and promotes mTORC1 kinase activity in its GTP-bound state (8–14).

Nutrient sensing is a key upstream signal for mTORC1 regulation, as growth factors or hormones are not sufficient to fully activate mTORC1 (9, 15). Whereas mTOR is dispersed within the cell upon amino acid starvation, amino acid replenishment redistributes mTOR to active, GTP-bound RHEB at the lysosomal surface (9). mTOR translocation is differentially regulated by the family of heterodimeric small Rag (Ras-related GTP binding) GTPases, which consists of four highly similar mammalian homologues (RagA, RagB, RagC, and RagD) (9, 16–19). Recruitment of mTOR to the lysosome is promoted by GTP-bound RagA/B and GDP-bound RagC/D, whereas it is inhibited by GDP-bound RagA/B and GTP-bound RagC/D (20). In turn, Rag proteins themselves are regulated by GAPs and guanine nucleotide exchange factors (GEFs). While the GATOR1 (GAP activity toward Rags) complex exhibits GAP activity toward RagA/B (21), FLCN (folliculin) and its interacting partners, FNIP1 (folliculin-interacting protein 1) and FNIP2, act on RagC/D (20). In addition, LRS (leucyl-tRNA synthetase) specifically stimulates GTP hydrolysis of RagD (22). The respective Rag GEF complex, termed Ragulator, is composed of 5 subunits (LAMTOR1 to -5) and executes GEF activity toward RagA/B (23). Additionally, Ragulator anchors Rag heterodimers to the lysosomal surface via its myristoylated subunit, LAMTOR1/p18 (16, 23). The binding capabilities of the Rag proteins to their respective GAPs or GEFs are influenced by the cellular amino acid status. For example, amino acid supply promotes LRS interaction with RagD, leading to its GTP hydrolysis and the subsequent increase in lysosomally localized and activated mTORC1 (22). In contrast, the interaction between Rag proteins and Ragulator subunits or folliculin-FNIP1/2 is strengthened upon amino acid starvation, while mTORC1 kinase activity is inhibited (16, 20). Furthermore, depletion of GATOR1 leads to mTORC1 hyperactivation and renders cells resistant to amino acid removal (21). In addition, lysosomal translocation and activation of mTORC1 upon amino acid stimulation requires the vacuolar H^+-ATPase ATPase (v-ATPase), which hydrolyzes ATP to produce a proton gradient across the lysosomal membrane and binds Ragulator in an amino acid-sensitive manner (24). Besides these recent advances in our understanding of this complex signaling cascade, the exact mechanism by which amino acids are sensed to control mTORC1 remains elusive.

We identified SLC38A9, a predicted 11-pass membrane protein and member of the solute carrier family 38 (SLC38) of sodium-coupled amino acid transporters, as a component of the

Received 3 February 2015 **Returned for modification** 1 March 2015
Accepted 30 April 2015

Accepted manuscript posted online 11 May 2015

Citation Jung J, Genau HM, Behrends C. 2015. Amino acid-dependent mTORC1 regulation by the lysosomal membrane protein SLC38A9. Mol Cell Biol 35:2479–2494. doi:10.1128/MCB.00125-15.

Address correspondence to Christian Behrends, behrends@em.uni-frankfurt.de.

Supplemental material for this article may be found at http://dx.doi.org/10.1128/MCB.00125-15.

doi:10.1128/MCB.00125-15

Rag-Ragulator machinery. Interaction proteomics revealed the association of SLC38A9 with RRAGB, RRAGC, and most components of the Ragulator complex using overexpressed or endogenous proteins. While the 119-amino-acid (aa)-long cytoplasmic tail of SLC38A9 was sufficient to mediate these associations independent of the amino acid status of the cell, binding of full-length SLC38A9 to RRAGA and RRAGC was increased upon amino acid starvation. SLC38A9 localized with LAMP2 and RRAGC as well as LAMTOR2 and LAMTOR5 on lysosomes. SLC38A9 depletion by RNA interference (RNAi) decreased mTORC1 activity, as monitored by the phosphorylation status of mTORC1 substrates in fed and amino acid-replenished cells. SLC38A9 overexpression caused RHEB GTPase-dependent mTORC1 hyperactivation and rendered cells partly insensitive to amino acid starvation. Intriguingly, we observed increased lysosomal translocation of mTOR in amino acid-starved cells depleted of SLC38A9. During the preparation of this report, two papers reported the role of SLC38A9 as a new component of the Rag GTPase-Ragulator amino acid-sensing machinery (25, 26). Through extensive biochemical studies, Rebsamen et al. and Wang et al. demonstrated that SLC38A9 is an amino acid transporter and regulates amino acid-dependent mTORC1 activity via the Rag-Ragulator complex (25, 26). Thus, we are the third group independently confirming and extending these findings. Collectively, we propose that SLC38A9 controls mTORC1 activity through binding to the Rag-Ragulator complex at the lysosome upon amino acid availability.

MATERIALS AND METHODS

Antibodies. Antibodies used included anti-4EBP1 (9644; Cell Signaling); anti-phospho-4EBP1 (Ser65) (9451; Cell Signaling); anti-Deptor (11816; Cell Signaling); anti-green fluorescent protein (anti-GFP) (11814460001; Roche); anti-hemagglutinin (anti-HA) (MMS-101P [Covance] and 11867423001 [Roche]); anti-LAMP2 (ab25631; Abcam); anti-mTOR (2983; Cell Signaling); anti-myc (sc-40; Santa Cruz); anti-RRAGB (8150; Cell Signaling); anti-RRAGA, anti-RRAGC, and anti-LAMTOR2 (Rag and LAMTOR antibody sampler kit; 8665; Cell Signaling); anti-PCNA (sc-7907; Santa Cruz); anti-S6K (9202; Cell Signaling); anti-phospho-S6K(Thr389) (9234; Cell Signaling); anti-SLC38A9 (HPA043785; Sigma-Aldrich); anti-ULK1 (8054; Cell Signaling); and anti-phospho-ULK1(Ser757) (6888; Cell Signaling).

Plasmids. PCR products generated from open reading frames (ORFs) (obtained from the human ORFeome collection) were cloned into the Gateway pDONR223 entry vector. PCR was used for the mutagenesis of plasmids (RRAGB Q99L, RRAGB T75L, RRAGC Q120L, and RRAGC S54L) according to the manufacturer's instructions (KOD hot start DNA polymerase; Merck Millipore). After sequence verification, cDNAs were subcloned into Gateway destination vectors for mammalian expression. The pHAGE-N-Flag-HA, MSCV-i(N-Flag-HA)-IRES-PURO, pDEST-MYC, and pHAGE-N-GFP vectors were used for transient transfection of 293T cells. Stable 293T-REx or 293T cells were generated by retroviral transduction of MSCV-i(N-Flag-HA)-IRES-PURO or lentiviral transduction of a GIPZ nonsilencing short hairpin RNA (shRNA) control (RHS4346; GE Healthcare), GIPZ shRHEB 1 (GGGTGATCAGTTATGA AGA), or GIPZ shRHEB 2 (TCAGACATACTCCATAGAT), followed by selection with antibiotics.

Cell culture. HEK-293T or HEK-293T-REx cells were cultured in Dulbecco's modified Eagle's medium (DMEM) supplemented with 10% fetal bovine serum (FBS), 2 mM glutamine, and antibiotics and maintained at 37°C and 5% CO_2. Expression of HA-tagged proteins in 293T-REx cell lines was induced by the addition of doxycycline (4 μg/ml; Sigma) 24 to 48 h before harvesting. The following reagents were used: Torin1 (250 nM; Tocris) and cycloheximide (2 μg/ml; Calbiochem).

Amino acid starvation. Amino acid-free RPMI medium (RPMI 1640 medium without amino acids; Biomol) was prepared according to the manufacturer's instructions (pH 7.4). For amino acid starvation, cells were washed three times with and then incubated in amino acid-free RPMI medium for 50 min. When indicated, cells were stimulated with amino acids for 50 min (fed) or 10 min (replenishment) by the addition of amino acid-free RPMI medium supplemented with RPMI 1640 amino acid solution (50×; Biomol), such that the final amino acid concentration was the same as that in standard RPMI medium. For individual amino acid replenishment, amino acid-free RPMI medium was supplemented with glutamine (200 μM; Life Technologies), arginine (114 μM; Sigma), or leucine (38 μM; Sigma).

Transfection-based experiments. Cells were reverse transfected with short interfering RNAs (siRNAs) targeting human SLC38A9 (Life Technologies and Dharmacon) or control siRNA (Stealth RNAi siRNA negative control, Med GC [Life Technologies], and ON-TARGETplus nontargeting pool [Dharmacon]) using Lipofectamine RNAiMax (Life Technologies) according to the manufacturer's instructions and typically harvested 72 h after transfection. siRNA sequences were the following (5′ to 3′): SLC38A9 1, ACCATGATGGGAACATCTATACTAA (HSS135864); SLC38A9 2, ACACTGAAGGATACGGTAA (J-007337-17). Plasmids were transfected using Lipofectamine 2000 (Life Technologies) or PEI (polyethylenimine; Polysciences Europe GmbH) according to standard protocols.

Immunoblotting. Proteins were separated by SDS-PAGE (4 to 20% gels [Bio-Rad] or self-casted 8% and 12% gels) and transferred to nitrocellulose membranes (0.45 μm; NitroBind; Fisher Scientific). Membranes were blocked with TBS-T (20 mM Tris, 150 mM NaCl, 0.1% Tween 20) containing 5% bovine serum albumin (BSA) (Sigma) or 5% low-fat milk (Roth). Blots were incubated with primary antibodies in blocking buffer at 4°C overnight, and secondary antibodies (anti-mouse antibody–horseradish peroxidase [HRP] [Promega], anti-rabbit antibody–HRP [Promega], anti-mouse IgG1(κ) [ab99617; Abcam], anti-mouse IgG1 heavy chain [ab97240; Abcam], and anti-rat antibody–HRP [Dianova]) were added for 1 h after washing with TBS-T.

IP. Expression of HA-tagged proteins was induced by the addition of 4 μg/ml doxycycline (Sigma) or by transient transfection. Forty-eight hours posttransfection or 24 h postinduction, cells were harvested and stored at −80°C. Cell pellets were lysed as indicated in ice-cold MCLB NP-40 buffer (50 mM Tris [pH 7.4], 150 mM NaCl, 0.5% NP-40), MCLB 3-[(3-cholamidopropyl)-dimethylammonio]-1-propanesulfonate (CHAPS) buffer (50 mM Tris [pH 7.4], 150 mM NaCl, 0.3% CHAPS), or HEPES buffer (1% NP-40, 50 mM HEPES, pH 7.4, 250 mM NaCl, 5 mM EDTA) supplemented with cOmplete EDTA-free protease inhibitor tablets (Roche) and phosphatase inhibitor (PhosSTOP; Roche) and incubated on ice for 30 min. Cell debris was removed from lysates by centrifugation, and the supernatant was subjected to immunoprecipitation (IP) with preequilibrated anti-HA–agarose (Sigma) or anti-GFP-resin (ChromoTek) overnight at 4°C. Afterwards, agarose beads were washed three times with MCLB buffer, and bound proteins were eluted by the addition of 4× Laemmli buffer with or without boiling at 95°C for 5 min. Samples then were analyzed by SDS-PAGE and immunoblotting.

Endogenous immunoprecipitation. 293T cells were lysed in HEPES buffer for 30 min on ice. Cell debris was removed by centrifugation, and lysates were precleared by the addition of protein A/G plus agarose beads (Santa Cruz) for 1 h at 4°C. Precleared lysates were incubated with the indicated antibodies overnight at 4°C, followed by the addition of agarose beads for 2 h. After washing with HEPES buffer three times, proteins were eluted by the addition of 4× Laemmli buffer and boiling at 95°C for 5 min. Proteins were separated by SDS-PAGE and analyzed by immunoblotting or subjected to in-gel trypsin digestion and mass spectrometry (MS) analysis.

MS-based proteomics. Expression of HA-tagged bait proteins in 293T-REx cells was induced for 24 h with 4 μg/ml doxycycline (Sigma) in four 15-cm cell culture dishes per condition. Cells were washed and harvested with ice-cold phosphate-buffered saline (PBS), followed by storage at −80°C or immediate lysis in 4 ml MCLB buffer. Cell debris was re-

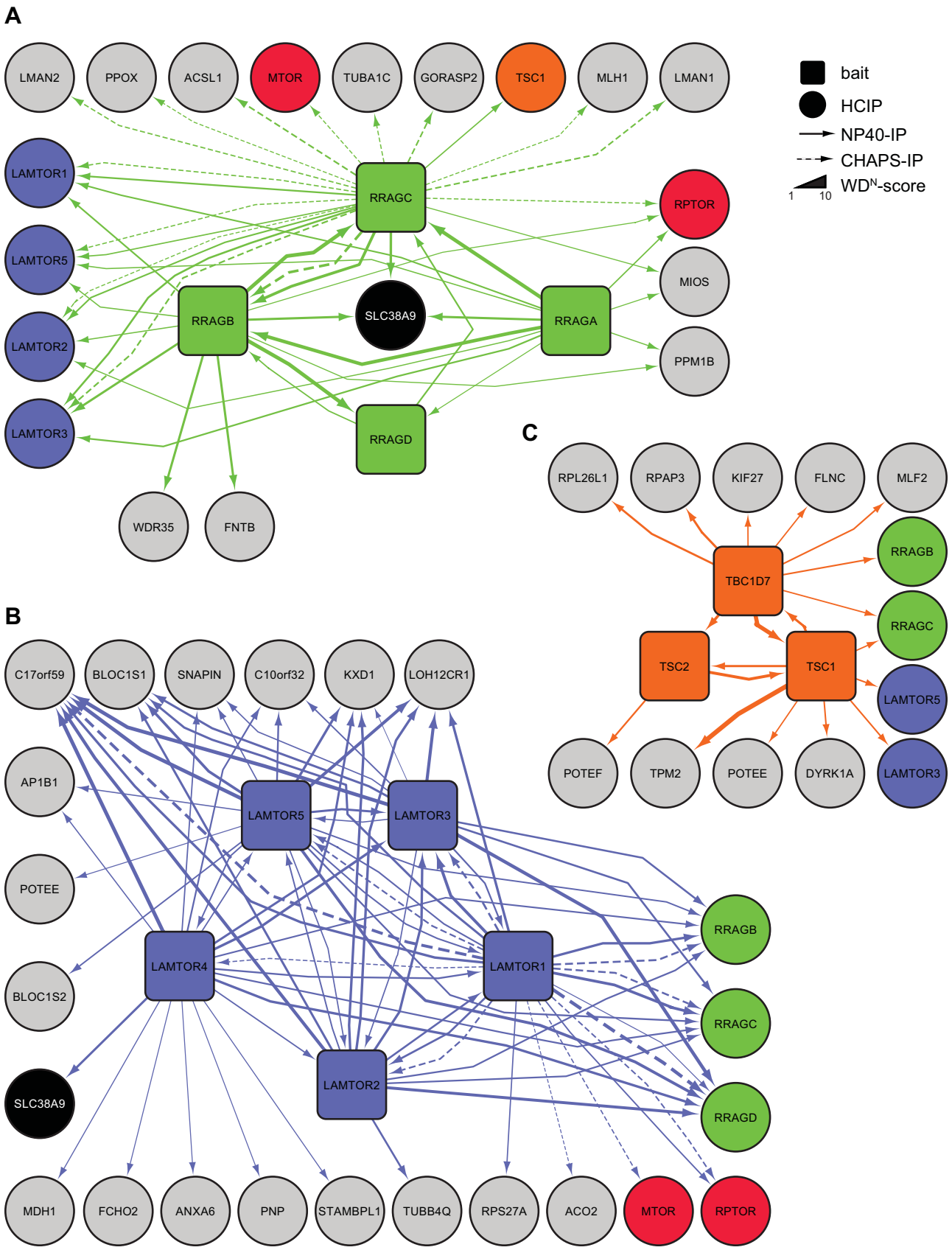

FIG 1 Interaction proteomics of regulatory mTORC1 components. (A to C) Grouped interaction network schemes obtained by IP-MS analysis of 12 baits consisting of the Rag GTPases (A), all Ragulator subunits (B), and TSC (C) and their high-confidence candidate interacting proteins (HCIPs; average APSM of ≥3 and WD^N score of ≥1). All interactions are color-coded according to functional group (red, mTORC1; blue, Ragulator; green, Rag proteins; orange, TSC; black, SLC38A9). Line thickness indicates interactions with WD^N scores between 1 and 10. Differential lysis with MCLB NP-40 (solid lines) or MCLB CHAPS (dashed lines) buffer is indicated. See Table S1A and B and Fig. S1 in the supplemental material for complete proteomic data.

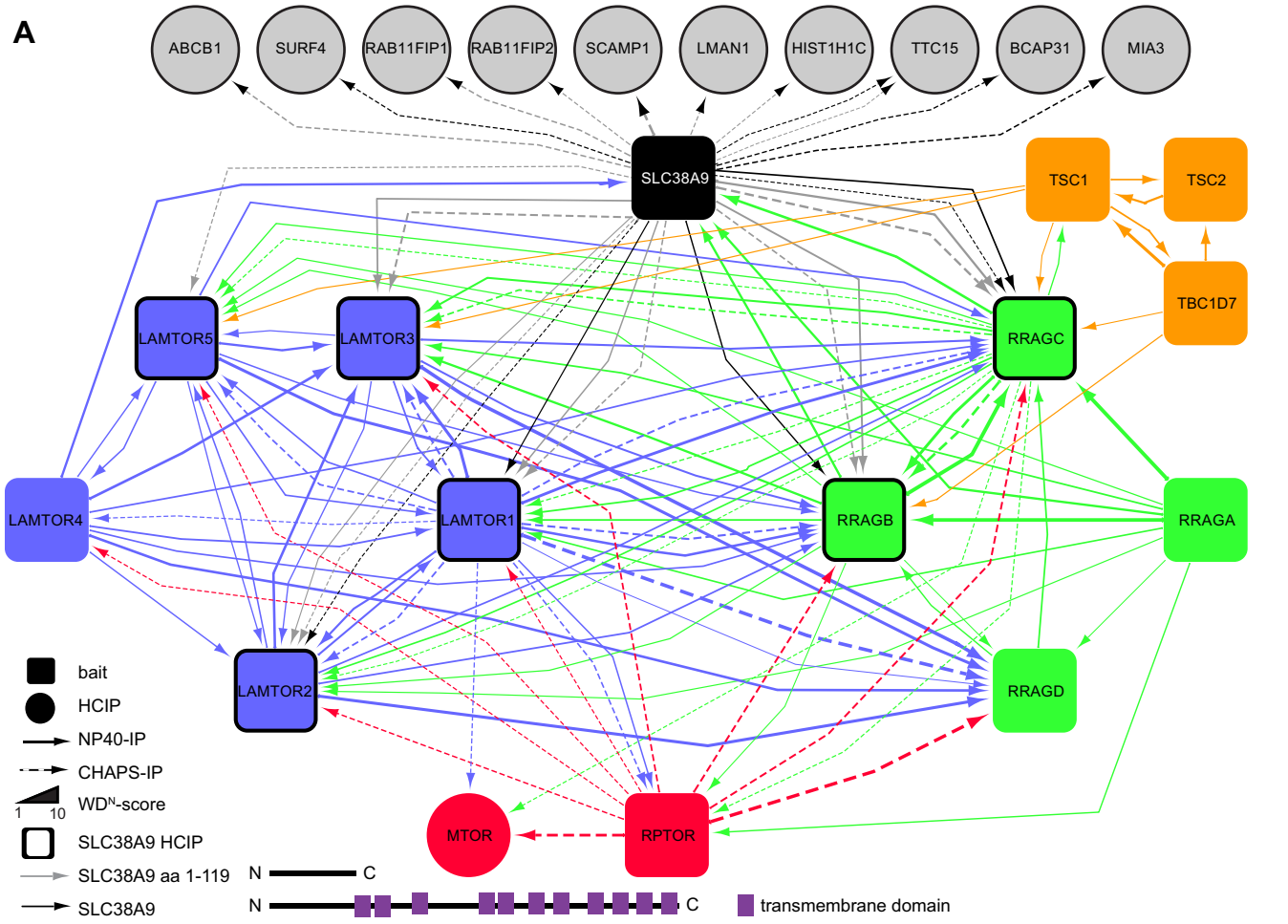
A
ABCB1
SURF4
RAB11FIP1
RAB11FIP2
SCAMP1
LMAN1
HIST1H1C
TTC15
BCAP31
MIA3
SLC38A9
TSC1
TSC2
TBC1D7
LAMTOR5
LAMTOR3
RRAGC
LAMTOR4
LAMTOR1
RRAGB
RRAGA
LAMTOR2
RRAGD
MTOR
RPTOR
bait
HCIP
NP40-IP
CHAPS-IP
WDN-score
1
10
SLC38A9 HCIP
SLC38A9 aa 1-119
SLC38A9
N
C
N
C
transmembrane domain

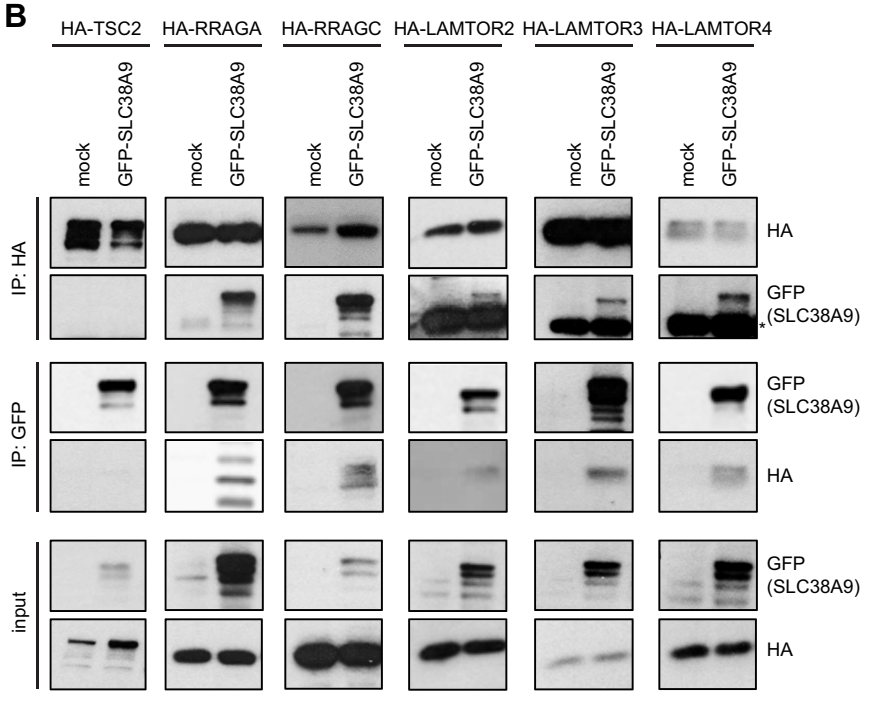
B
HA-TSC2
HA-RRAGA
HA-RRAGC
HA-LAMTOR2
HA-LAMTOR3
HA-LAMTOR4
mock
GFP-SLC38A9
IP: HA
IP: GFP
input
HA
GFP (SLC38A9)
GFP (SLC38A9)
HA
GFP (SLC38A9)
HA
*

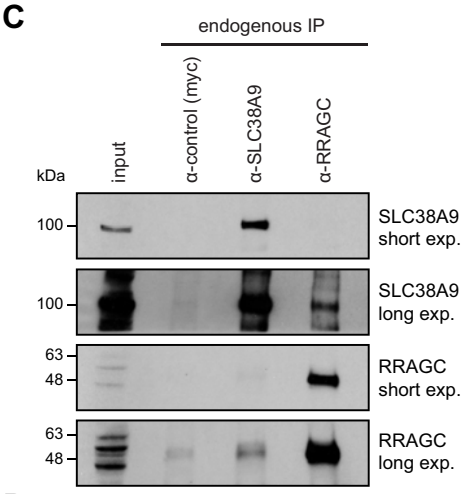
C
endogenous IP
kDa
input
α-control (myc)
α-SLC38A9
α-RRAGC
100
100
63
48
63
48
SLC38A9 short exp.
SLC38A9 long exp.
RRAGC short exp.
RRAGC long exp.

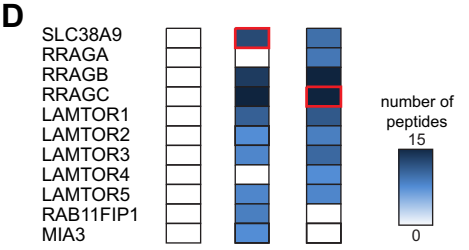
D
SLC38A9
RRAGA
RRAGB
RRAGC
LAMTOR1
LAMTOR2
LAMTOR3
LAMTOR4
LAMTOR5
RAB11FIP1
MIA3
number of peptides
15
0

moved from the lysates by centrifugation, and supernatants were passed through 0.45-μm spin filters (Millipore). Anti-HA–agarose (60-μl slurry; Sigma) was added to lysates for immunoprecipitation overnight, with rotation, at 4°C. Samples were washed five times with 1 ml MCLB, followed by five washes with PBS and elution with 150 μl HA peptide (250 μg/ml; Sigma). Eluted immune complexes were processed and analyzed essentially as previously described (27, 28). Briefly, proteins were precipitated with trichloroacetic acid (Sigma) followed by digestion with trypsin (Promega) and desalting by stage tips. Samples were analyzed in technical duplicates on an LTQ Velos (Thermo Scientific). Spectra were identified by Sequest searches, followed by target decoy filtering and linear discriminant analysis as described in reference 29. Peptides that could be assigned to more than one protein in the database were assembled into proteins according to parsimony principles. For CompPASS analysis, we employed 215 unrelated bait proteins that all were previously processed in the same way (27, 28). Weighted and normalized D scores (WD^N scores) were calculated based on average peptide spectral matches (APSMs). Proteins with WD^N of ≥1 and APSM of ≥3 were considered high-confidence candidate interacting proteins (HCIPs).

In-gel trypsin digestion. After SDS-PAGE, gels were silver stained (SilverQuest staining kit; Life Technologies) according to the manufacturer's instructions, and then whole lanes were cut and washed three times with 50 mM ammonium bicarbonate (ABC) containing 50% acetonitrile (ACN), followed by dehydration for 10 min with ACN and reduction for 45 min at 56°C with 10 mM dithiothreitol (DTT) in 20 mM ABC. For alkylation, gel pieces were incubated with 55 mM iodoacetamide in 20 mM ABC for 30 min in the dark and then washed two times with 5 mM ABC containing 50% ACN, followed by dehydration with ACN and vacuum centrifugation. Subsequently, gel pieces were incubated with 12.5 ng/μl trypsin in 20 mM ABC overnight and eluted three times with increasing ACN concentrations. Desalting by stage tips and mass spectrometric analysis were performed on an LTQ Velos. Spectra were identified as described above.

RNA isolation, cDNA synthesis, and RT-qPCR. Total RNA from 293T cells was isolated using a High Pure RNA isolation kit (Roche) and then reverse transcribed into cDNA with a Transcriptor first-strand cDNA synthesis kit (Roche). Real-time quantitative PCR (RT-qPCR) was performed on a LightCycler 480 (Roche) employing LightCycler 480 SYBR green I master with specific primers for SLC38A9 (qPCR_SLC38A9_for, CAGTTTGAGCC ATCGGATCT; qPCR_SLC38A9_rev, GGTGAGCCGGCTGTAGTAAT) or RHEB GTPase (qPCR_RHEB_for, TACCGGTCTGTGGGGAAATC; qPCR_RHEB_rev, TATTCATCTTGCCCGGCTGT). Relative SLC38A9 or RHEB mRNA expression was normalized to the geometrical mean of three reference genes (ACTB, HMBS, and TBP; qPCR_ACTB_for, CG GGAAATCGTGCGTGACATTAAG; qPCR_ACTB_rev, TGATCTCC TTCTGCATCCTGTCGG; qPCR_HMBS_for, CCCTGGAGAAGAAT GAAGTGG; qPCR_HMBS_rev, TTCTCTGGCAGGGTTTCTAGG; qPCR_TBP_for, CACCTTACGCTCAGGGCTT; qPCR_TBP_rev, TA TTGGTGTTCTGAATAGGCTGTG).

Immunofluorescence. 293T or 293T-REx cells were seeded on poly-L-lysine-coated 384-well plates (PerkinElmer) and fixed with 4% paraformaldehyde after siRNA or plasmid transfections. Cells were permeabilized with 0.5% Triton X-100 in PBS (10 min), followed by blocking with 1% BSA in PBS for 1 h. Primary and secondary antibodies, as well as nuclear and cytoplasmic staining reagents (Alexa fluor-coupled antibodies; Life Technologies), anti-rat antibody–Cy3 (Jackson ImmunoResearch), DRAQ5 (Cell Signaling), and HSC CellMask deep-red stain (Life Technologies), were incubated in 0.1% BSA in PBS for 1 h with three washes of PBS in between. For double stainings, antibodies were incubated sequentially. Images were acquired on PerkinElmer's Opera high-content screening system with a 60× water immersion objective and visualized with Acapella high-content imaging analysis software (PerkinElmer). To assess mTOR translocation, the number of mTOR- or LAMP2-positive spots per cell were automatically counted using Acapella software. For the calculation of Pearson's correlation coefficient, pixel intensity in different channels of the overlay image was measured along a line in ImageJ and analyzed with GraphPad Prism and Excel.

Statistical analysis. Data represent means ± standard errors of the means (SEM), and statistical analysis was performed using GraphPad Prism. Statistical significance was determined with two-way analysis of variance (ANOVA) followed by Bonferroni's *post hoc* test.

RESULTS

SLC38A9 associates with the Rag-Ragulator complex. Given the complexity in the upstream regulation of mTORC1, we set out to systematically explore the cluster of regulatory components that control mTORC1 activity. To perform interaction proteomics within this metabolic checkpoint hub, we generated a panel of 293T-REx cells stably expressing inducible hemagglutinin (HA)-tagged subunits of Ragulator (LAMTOR1, LAMTOR2, LAMTOR3, LAMTOR4, and LAMTOR5), members of the Rag GTPases family (RRAGA, RRAGB, RRAGC, and RRAGD), TSC components (TSC1, TSC2, and TBC1D7), and the mTORC1 subunit Raptor. Lysates derived from these cells were subjected to parallel HA-immunoprecipitations (IP), followed by peptide elution, trypsin digestion, and analysis by liquid chromatography-tandem mass spectrometry (LC-MS/MS). Mass spectral data were processed using the CompPASS platform to identify high-confidence candidate interacting proteins (HCIPs) of each bait protein (27, 28) (Fig. 1A to C; also see Fig. S1 and Table S1A and B in the supplemental material). Raptor served as a quality control for our approach and was able to retrieve all known mTORC1 subunits, as well as mTORC1 substrates, with high confidence (see Fig. S1A). As expected, a high degree of reciprocal interconnectivity was detected between Rag and LAMTOR proteins using two different lysis buffer conditions (Fig. 1A and B, NP-40 [solid lines] and CHAPS [dashed lines]; also see Fig. S1B to J). In addition, Rag-Ragulator complex subunits were found associated with Raptor and TSC components (Fig. 1C; also see Fig. S1A and K to M). Conversely, several Ragulator members shared associations with the biogenesis of lysosome-related organelles complex 1 (BLOC-1) components BLOC1S1 and BLOC1S2, SNAPIN (SNAP-associated protein), and KXD1 (KxDL motif containing

FIG 2 SLC38A9 associates with the Rag-Ragulator complex. (A) Overview of the regulatory mTORC1 interaction network obtained by IP-MS analysis of 14 baits consisting of Raptor, TSC, LAMTOR1-5, and Rag GTPases, as well as SLC38A9. Functional groups and lysis buffer are coded as described in the legend to Fig. 1. SLC38A9 HCIPs are marked by black edging. Interactions with full-length SLC38A9 or its N-terminal fragment (aa 1 to 119) are indicated in black and gray, respectively. Schematic representation of the domain structure of SLC38A9 is provided. See Table S1A and B and Fig. S1 in the supplemental material for complete proteomic data. (B) 293T-REx cells inducibly expressing HA-tagged components of the Rag-Ragulator complex or TSC2 were transfected with GFP-SLC38A9 or left untransfected (mock). NP-40 cell lysates were subjected to immunoprecipitation with anti-GFP or anti-HA beads as indicated and analyzed by SDS-PAGE and immunoblotting. *, IgG heavy chain. (C and D) 293T cells were lysed with HEPES buffer followed by immunoprecipitation with anti-SLC38A9, anti-RRAGC, or anti-myc as a control. Coimmunoprecipitated proteins were separated by SDS-PAGE and analyzed by immunoblotting (C) or subjected to in-gel trypsin digestion and mass spectrometric analysis (D). The number of peptides is shown from 0 to 15 peptides per protein. Immunoprecipitated bait proteins are marked by red edging. See Table S1C in the supplemental material for complete proteomic data.

1), as well as with the uncharacterized proteins C17orf59, C10orf32, and LOH12CR1 (Fig. 1B). The Rag GTPase subnetwork revealed Raptor, the GATOR2 subunit MIOS, and the protein phosphatase 1B (PPM1B) as common interactors (Fig. 1A). Furthermore, RRAGC interacted with the two endoplasmic reticulum Golgi intermediate compartment (ERGIC)-localized proteins LMAN1 and LMAN2 (lectin mannose-binding 1 and 2, respectively), as well as with GORASP2 (Golgi reassembly stacking protein 2), a protein located at the Golgi membrane (Fig. 1A; also see Fig. S1J). Several transport proteins, like FLNC (filamin C) or KIF27 (kinesin family member 27), additionally were revealed in the TSC network (Fig. 1C; also see Fig. S1K to M).

Within the combined Raptor-TSC-Rag-LAMTOR interaction network, our attention was drawn to SLC38A9, which is a member of the solute carrier family 38 (SLC38) of sodium-coupled amino acid transporters. SLC38A9 was identified as the HCIP of RRAGA, RRAGB, and RRAGC, as well as of the Ragulator subunit LAMTOR4 (Fig. 1A and B; also see Fig. S1E, G, H, and J in the supplemental material). In addition, SLC38A9 also associated with LAMTOR1 and LAMTOR3, albeit without passing the strict threshold for HCIP determination (see Table S1A). Reciprocal IP-MS analysis of HA-tagged SLC38A9 confirmed the interaction with Rag GTPases and Ragulator components and revealed several other associating proteins which are known to be involved in vesicular transport, such as TTC15 (TPR repeat protein 15; also known as TRAPPC12 [trafficking protein particle complex 12]), SURF4 (surfeit 4), SCAMP1 (secretory carrier membrane protein 1), BCAP31 (B-cell receptor-associated protein 31), MIA3 (melanoma inhibitory activity family, member 3), and RAB11FIP1 (RAB11 family interacting protein 1 [class I]) and RAB11FIP2 (Fig. 2A). These proteins may participate in the trafficking of SLC38A9 from the endoplasmic reticulum to lysosomes.

To further validate the interaction of SLC38A9 with Rag and LAMTOR proteins, we performed a series of reciprocal immunoprecipitation experiments followed by immunoblotting. HA-tagged RRAGA, RRAGC, LAMTOR2, LAMTOR3, and LAMTOR4 efficiently pulled down GFP-tagged SLC38A9 and vice versa (Fig. 2B). TSC2, which is an upstream regulator of mTORC1 (30, 31), was employed as a negative control and did not associate with SLC38A9 (Fig. 2B). Immunoprecipitation with anti-SLC38A9 or anti-RRAGC antibodies confirmed the association of SLC38A9 and RRAGC at endogenous levels (Fig. 2C). Subsequent MS analysis further verified the endogenous interaction of SLC38A9 with almost all members of the Rag-Ragulator complex, as well as with MIA3 and RAB11FIP1 (Fig. 2D). Collectively, these data provide strong evidence that SLC38A9 associates tightly with components of the Rag-Ragulator complex.

The cytosolic tail of SLC38A9 is sufficient to mediate association with the Rag-Ragulator complex. SLC38A9 is predicted to encompass 11 transmembrane domains (32) and a 119-aa-long N-terminal tail that faces the cytoplasm (Fig. 2A). To determine which part of SLC38A9 mediates association with Rag and LAMTOR proteins, we transiently expressed full-length SLC38A9 and the N-terminal cytosolic fragment (aa 1 to 119) as GFP fusions in stable 293T-REx cells inducibly expressing HA-tagged Rag or LAMTOR proteins. Immunoprecipitation experiments demonstrated that binding of SLC38A9 to RRAGA, RRAGB, and LAMTOR1 was retained or even enhanced only when the N-terminal fragment was employed (Fig. 3). We also subjected lysates derived from cells inducibly expressing the N-terminal cytosolic

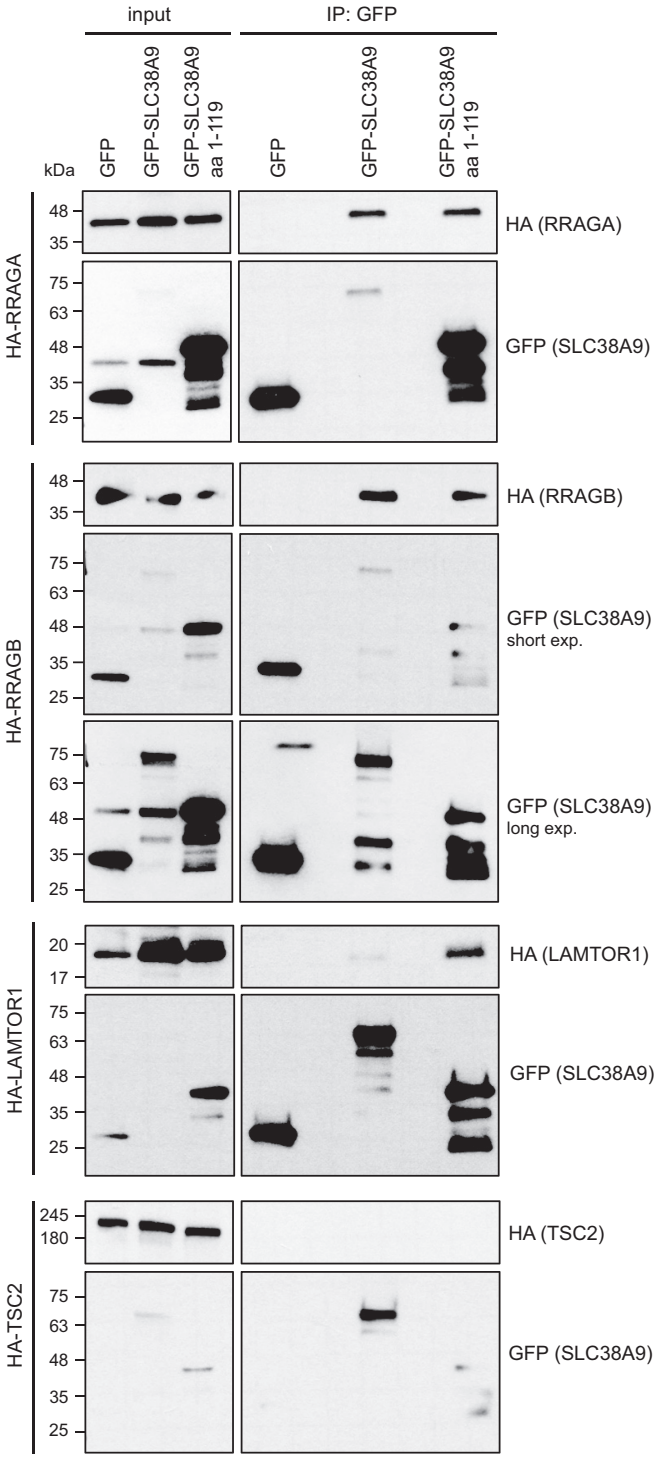

FIG 3 Cytosolic N terminus of SLC38A9 mediates association with the Rag-Ragulator complex. 293T-REx cells inducibly expressing the indicated HA-tagged Rag or LAMTOR proteins were transfected with GFP-SLC38A9 full length, GFP-SLC38A9 aa 1 to 119, or GFP alone. NP-40 cell lysates were subjected to immunoprecipitation with anti-GFP beads, and coimmunoprecipitated proteins were detected by SDS-PAGE and immunoblotting.

fragment of SLC38A9 to IP-MS analysis. LAMTOR1, LAMTOR2, LAMTOR3, and LAMTOR5, as well as RRAGB and RRAGC, associated with the first 119 amino acids of SLC38A9 (Fig. 2A, gray arrows). Thus, these results suggest that the N-terminal soluble

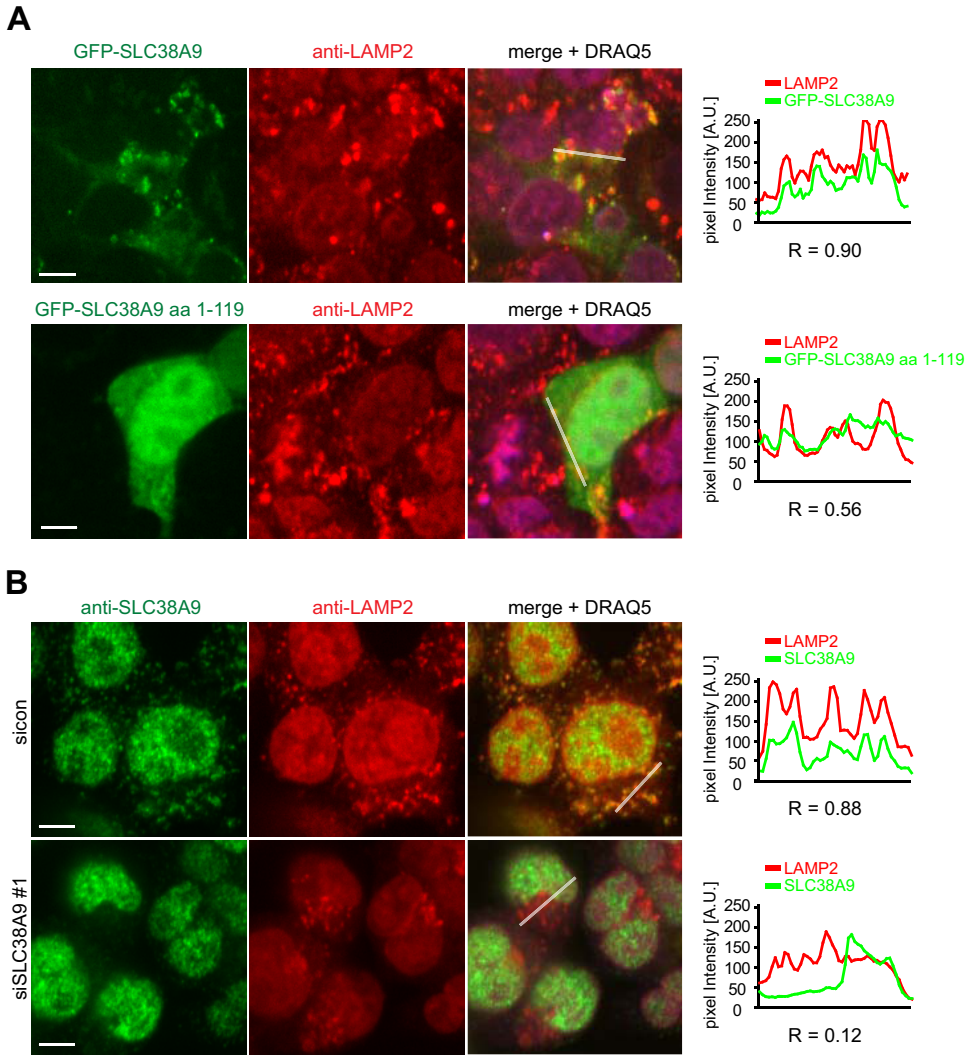

FIG 4 SLC38A9 localizes to lysosomes. (A) 293T cells transfected with GFP-SLC38A9 full length or GFP-SLC38A9 aa 1 to 119 were fixed and stained with anti-LAMP2 antibody. Scale bar, 10 μm. Pearson's correlation coefficient (*R*) was calculated in Excel after measuring pixel intensity in different channels of the overlay image along a line in ImageJ. A.U., arbitrary units. (B) 293T cells transfected with nontargeting control (sicon) or *SLC38A9* siRNA were fixed and labeled with anti-SLC38A9 and anti-LAMP2 antibodies. Scale bar, 10 μm. *R* was calculated as described for panel A.

part of SLC38A9 is sufficient for associating with several subunits of the Rag-Ragulator complex.

SLC38A9 localizes to lysosomes. Given that SLC38A9 associates with Rag and LAMTOR proteins, which peripherally reside on lysosomes, we examined the subcellular localization of SLC38A9. While GFP-tagged SLC38A9 localized to LAMP2-positive vesicles with strong positive correlation (Pearson's correlation coefficient [*R*] of 0.9), the N-terminal fragment lacking all transmembrane domains was dispersed mainly in the cytosol and the nucleus (Fig. 4A). However, a small fraction of GFP-tagged SLC38A9 (aa 1 to 119) also colocalized to LAMP2-positive vesicles still maintaining intermediate positive correlation ($R = 0.56$), possibly due to interactions with components of the Rag-Ragulator complex (Fig. 4A). Moreover, endogenous SLC38A9 and LAMP2 were detected together in punctuated vesicular structures throughout the cytosol with strong positive correlation ($R = 0.88$) (Fig. 4B). Notably, RNAi-mediated depletion of SLC38A9 revealed that this vesicular staining of the antibody was specific for SLC38A9 (Fig. 4B) with no correlation between the remaining unspecific nuclear staining of SLC38A9 and LAMP2 ($R = 0.12$). Thus, SLC38A9 is a lysosomal transmembrane protein.

Localization and association of SLC38A9 with the Rag-Ragulator complex are differentially affected by amino acids. Since Rag GTPases and Ragulator regulate mTORC1 activity in an amino acid-dependent manner, we monitored the dynamics of SLC38A9 localization and associations with components of the Rag-Ragulator complex in amino acid-starved (amino acid starvation medium) and fed (amino acid starvation medium complemented with amino acids) conditions. Confocal microscopy revealed that endogenous SLC38A9 colocalized with HA-tagged RRAGC, LAMTOR2, and LAMTOR5, as well as with endogenous LAMP2, irrespective of the cellular amino acid status and with strong positive correlation ($0.82 \leq R \leq 0.97$) (Fig. 5). The specificity of the vesicular SLC38A9 staining was confirmed by siRNA-mediated depletion of SLC38A9, which dramatically decreased the correlation ($-0.65 \leq R \leq 0.20$) (Fig. 5). Notably, amino acid

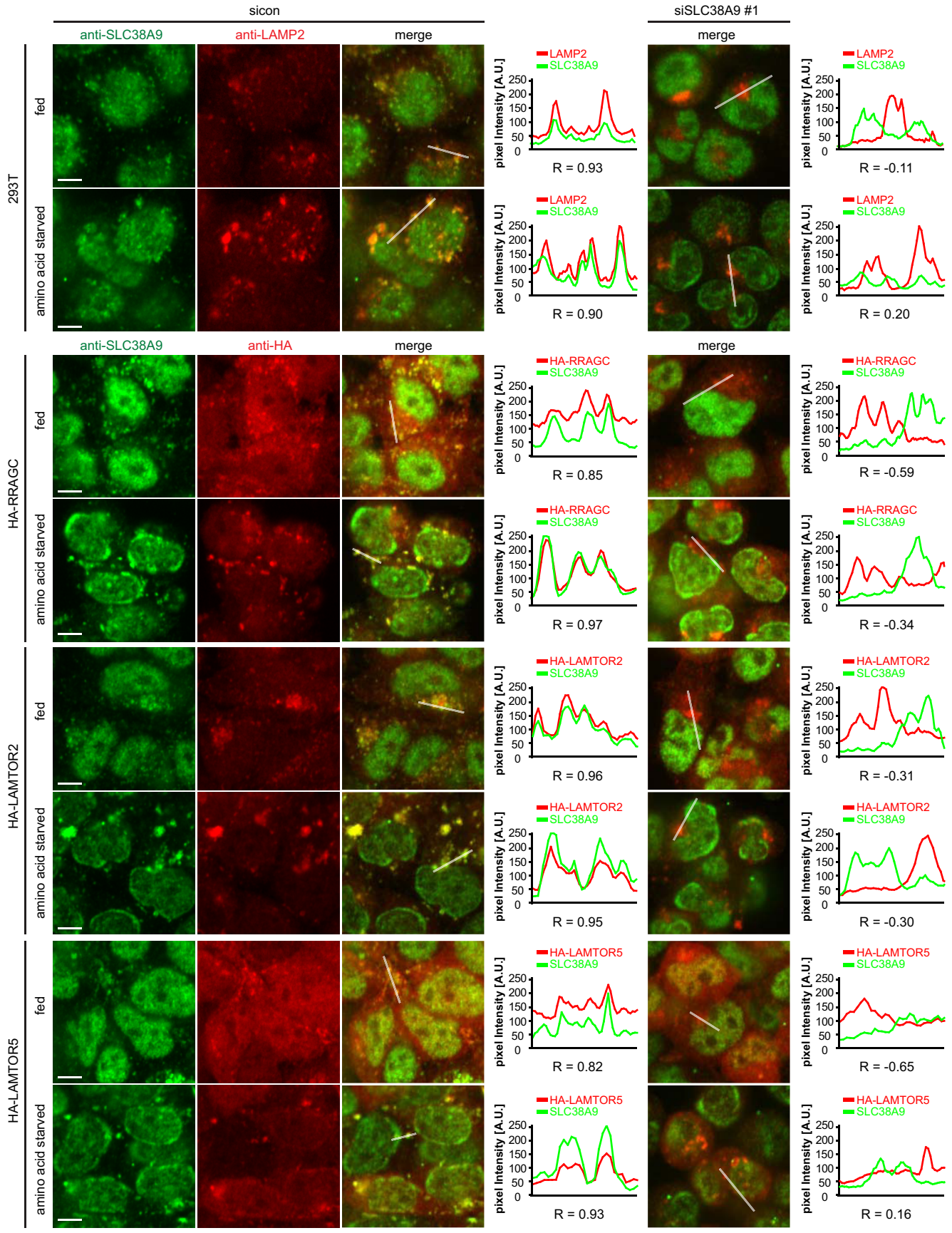

FIG 5 Amino acid-independent colocalization of SLC38A9 with the Rag-Ragulator complex. 293T or 293T-REx cells inducibly expressing HA-tagged components of the Rag-Ragulator complex were transfected with control (sicon) or *SLC38A9* siRNA. Prior to fixation and labeling with anti-HA or anti-LAMP2 and anti-SLC38A9 antibody, cells were cultured for 50 min in full RPMI growth medium (fed) or amino acid starved. Scale bar, 10 μm. Pixel intensity was measured in different channels of the overlay image along a line in ImageJ, and Pearson's correlation coefficient (*R*) was calculated in Excel.

starvation induced clustering of LAMP2 (33)- and SLC38A9-positive lysosomes, and overexpressed HA-RRAGC, HA-LAMTOR2, and HA-LAMTOR5 colocalized to these clusters (Fig. 5).

Immunoprecipitation experiments showed that interaction of GFP-tagged full-length SLC38A9 with HA-tagged RRAGA and RRAGC was markedly enhanced upon amino acid starvation. In contrast, binding of GFP-tagged SLC38A9 aa 1 to 119 to HA-RRAGA and HA-RRAGC was amino acid insensitive (Fig. 6A). As described for other Rag GTPase-interacting proteins (20, 23), binding of SLC38A9 to RRAGA/RRAGC or RRAGB/RRAGC heterodimers was dependent on their nucleotide states. While the Rag GTPase mutants RRAGB-Q99L and RRAGC-S54L, which are locked in the mTORC1 activating nucleotide states, completely abolished the amount of coimmunoprecipitated SLC38A9 compared to that of wild-type RRAGB/RRAGC, binding of SLC38A9 was increased when the Rag GTPase mutants RRAGB-T75L and RRAGC-Q120L, which are locked in the nucleotide binding state, were used (Fig. 6B). Notably, SLC38A9 preferred binding to RRAGA/RRAGC over pairing with RRAGB/RRAGC (Fig. 6B). Overexpressed myc-tagged LAMTOR2 was found to be increasingly associated with wild-type RRAGB/RRAGC and mutant RRAGB-T75L/RRAGC-Q120L heterodimers in RNAi-mediated, SLC38A9-depleted cells (Fig. 6B). Importantly, SLC38A9 depletion had no effect on the composition of Ragulator, Rag GTPase, and mTORC1 complexes (Fig. 6C to E; also see Table S1D in the supplemental material). Thus, SLC38A9 localizes with the Rag-Ragulator complex at lysosomes irrespective of the nutritional conditions, while the interaction between SLC38A9 and Rag GTPases is determined by their nucleotide binding state and additionally strengthened upon amino acid starvation dependent on the transmembrane domain of SLC38A9.

SLC38A9 is required for mTORC1 signaling. We next examined whether mTORC1 kinase activity was regulated by SLC38A9. In SLC38A9-depleted cells, phosphorylation of the mTORC1 substrates S6K (ribosomal protein S6 kinase; 70-kDa, polypeptide 1), 4EBP1 (eukaryotic translation initiation factor 4E binding protein 1), and ULK1 (unc-51-like autophagy activating kinase 1) was decreased, whereas their total protein levels remained unchanged (Fig. 7A and B). Notably, knockdown of SLC38A9 was confirmed by immunoblotting (Fig. 7A and B) and RT-qPCR (Fig. 7C). In contrast, we observed increased phosphorylation of S6K and ULK1 when full-length SLC38A9 or its N-terminal fragment was overexpressed (Fig. 7D). Importantly, the hyperactivity of mTORC1 induced by SLC38A9 overexpression was completely abolished when cells were treated with the catalytic mTOR inhibitor Torin1 (Fig. 7E) and substantially reduced when the GTPase RHEB was specifically depleted (Fig. 7F), indicating that SLC38A9-mediated mTORC1 activation is achieved through RHEB. Depletion of RHEB was confirmed by RT-qPCR (Fig. 7G). Together, our data and the homology of SLC38A9 to other SLC38 class proteins (34) raise the possibility that the lysosomal transmembrane protein SLC38A9 functions to control mTORC1 kinase activity in an amino acid-sensitive manner.

SLC38A9 regulates mTORC1 activity upon amino acid availability. To test our hypothesis, we monitored mTORC1 activity in response to altered amino acid homeostasis in SLC38A9-depleted or overexpressing cells. First, we treated cells with cycloheximide (CHX), which is known to increase the intracellular pool of amino acids (35–37). As expected, phosphorylation of ULK1 and 4EBP1 increased upon CHX treatment. However, depletion of SLC38A9 inhibited this effect completely (Fig. 8A). Second, we incubated cells shortly (50 min) in the absence of amino acids. Compared to fed cells, phosphorylation of ULK1 decreased upon amino acid starvation (Fig. 8B). In contrast, amino acid starvation did not aggravate the reduced ULK1 phosphorylation observed in SLC38A9-depleted cells (Fig. 8B). Consistent with this, the overexpression of SLC38A9 partially reverted the amino acid starvation-induced decrease in ULK1 phosphorylation (Fig. 8C). Third, following a short period of amino acid starvation, we replenished all amino acids or individual amino acids known to regulate mTORC1 activity, namely, glutamine, arginine, or leucine (15, 38, 39). In siRNA control cells, phosphorylation of ULK1 increased under all replenishment conditions. However, in SLC38A9-depleted cells, ULK1 phosphorylation only marginally increased upon amino acid replenishment irrespective of whether all or only individual amino acids were used (Fig. 8D). In sum, we provide evidence that altered SLC38A9 protein levels render cells partly insensitive to amino acid availability.

SLC38A9 is required for mTOR relocation from lysosomes to the cytosol. In amino acid-starved cells, mTOR is dispersed throughout the cytoplasm, while amino acid replenishment stimulates mTOR recruitment from the cytoplasm to the lysosomal surface (9). Hence, we tested whether SLC38A9 depletion influenced the lysosomal localization of mTOR upon amino acid availability. Relocation of mTOR to the cytoplasm was induced by amino acid starvation (Fig. 9A to C). Intriguingly, mTOR was significantly retained on LAMP2-positive lysosomal clusters upon SLC38A9 knockdown in the presence and absence of amino acids. Depletion of Raptor served as a positive control causing cytosolic mTOR localization (Fig. 9A and B). Notably, SLC38A9 depletion had no effect on the number of lysosomes (Fig. 9D) or the protein abundance of LAMP2 (Fig. 9E). Thus, these results suggest that SLC38A9 is required to release inactivated mTORC1 from lysosomal membranes (Fig. 9F).

DISCUSSION

Regulation of mTORC1 by amino acids has been studied extensively, and a growing number of proteins contribute to control activity and/or localization of mTORC1. Depending on their nucleotide binding state, Rag GTPases recruit mTORC1 to the lysosome, where mTORC1 activity is stimulated via the GTPase RHEB (9, 13, 16), while Ragulator recruits and anchors the Rag GTPases to the lysosome (16). Further on, interactions between Rag and LAMTOR proteins, as well as between Rags and their GAPs and GEFs, are dependent on the cellular amino acid status. Recently, the amino acid transporter SLC38A9 has been identified as an additional component of the Rag-Ragulator complex (25, 26). mTORC1 activation was reported to be abolished in SLC38A9 knockout cells (26), while SLC38A9 overexpression caused mTORC1 hyperactivation even during amino acid starvation (25, 26).

In this study, we systematically employed interaction proteomics to identify novel proteins associating with the network of amino acid-sensitive mTORC1 regulators. SLC38A9, an 11-pass membrane protein and member of the solute carrier family 38 (SLC38) of sodium-coupled amino acid transporters, reciprocally associated with several components of the Rag-Ragulator complex. While the 119-aa-long N-terminal cytosolic tail that precedes the transmembrane part of SLC38A9 was sufficient to mediate interaction with Rag GTPases and Ragulator, full-length

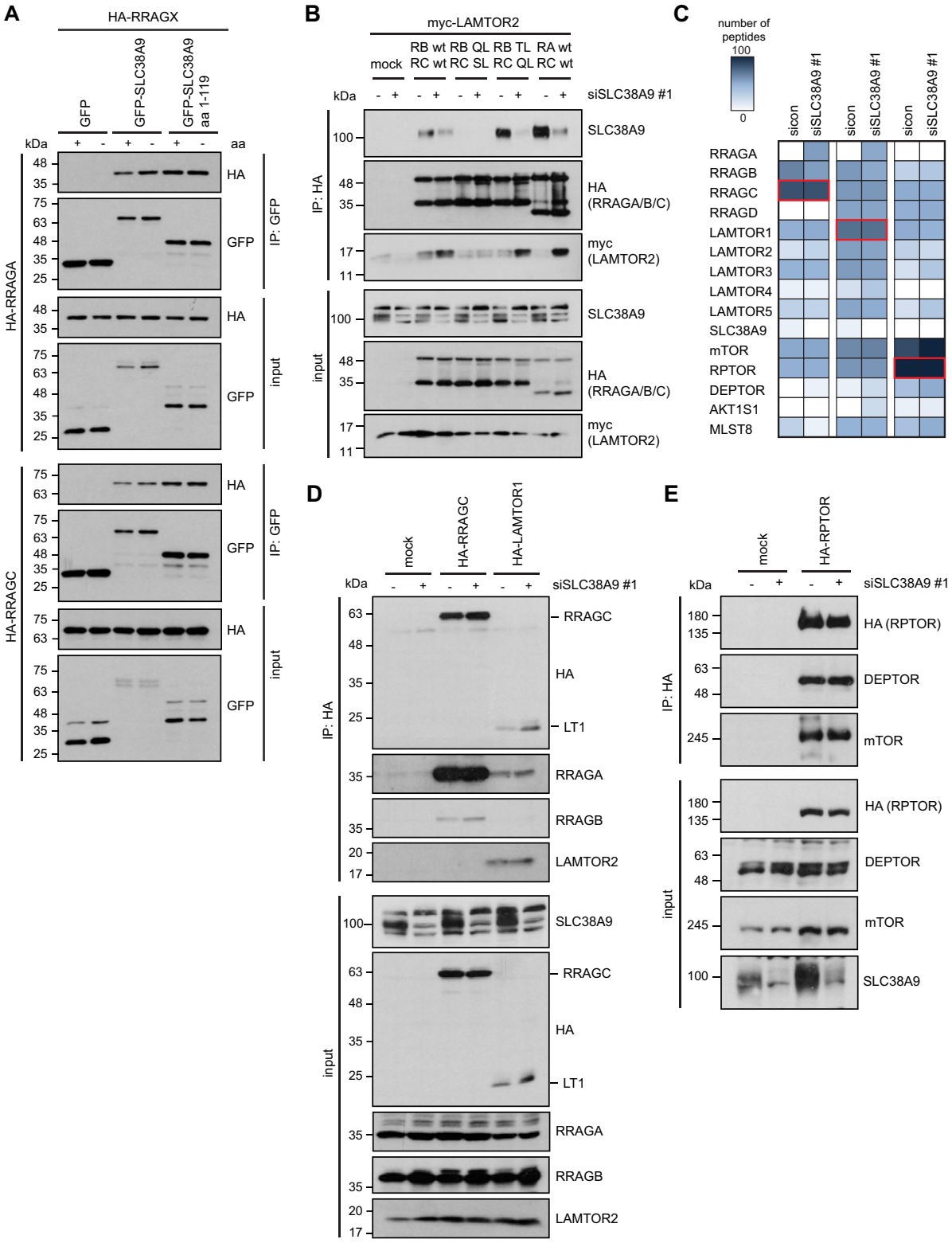

FIG 6 Association of SLC38A9 with Rag GTPases is amino acid and nucleotide dependent. (A) 293T-REx cells inducibly expressing HA-tagged Rag GTPase proteins were transfected with GFP-SLC38A9 full length, GFP-SLC38A9 aa 1 to 119, or GFP alone. Cells were either grown for 50 min in full RPMI growth medium (fed) or were amino acid (aa) starved and subsequently lysed with MCLB NP-40 for GFP immunoprecipitation. Immunoprecipitates were analyzed by SDS-PAGE and immunoblotting. (B) 293T cells were transfected with nontargeting control (sicon) or *SLC38A9* siRNAs and myc-tagged LAMTOR2, as well as wild-type (RRAGB wild-type [RB wt], RRAGC wild-type [RC wt], RRAGA wild type [RA wt]) or mutant (RRAGB Q99L [RB QL], RRAGB T75L [RB TL], RRAGC Q120L [RC QL], RRAGC S54L [RC SL]) HA-tagged Rag GTPase proteins, as indicated. Cells were lysed in HEPES buffer, subjected to HA-immunoprecipitation, and analyzed as described above. (C) 293T-REx cells inducibly expressing HA-tagged RRAGC, LAMTOR1, or Raptor (marked with red edging) were transfected with control (sicon) or *SLC38A9* siRNA as indicated, followed by lysis in MCLB CHAPS buffer and immunoprecipitation with HA beads. Eluates were analyzed by MS. The number of peptides is shown from 0 to 100 peptides per protein. See Table S1D in the supplemental material for complete proteomic data. (D) Cells like those described for panel C were lysed in HEPES buffer followed by immunoprecipitation, SDS-PAGE, and immunoblotting. (E) Raptor overexpressing 293T-REx cells were transfected as described for panel C, lysed in MCLB CHAPS buffer, and analyzed as described for panel D.

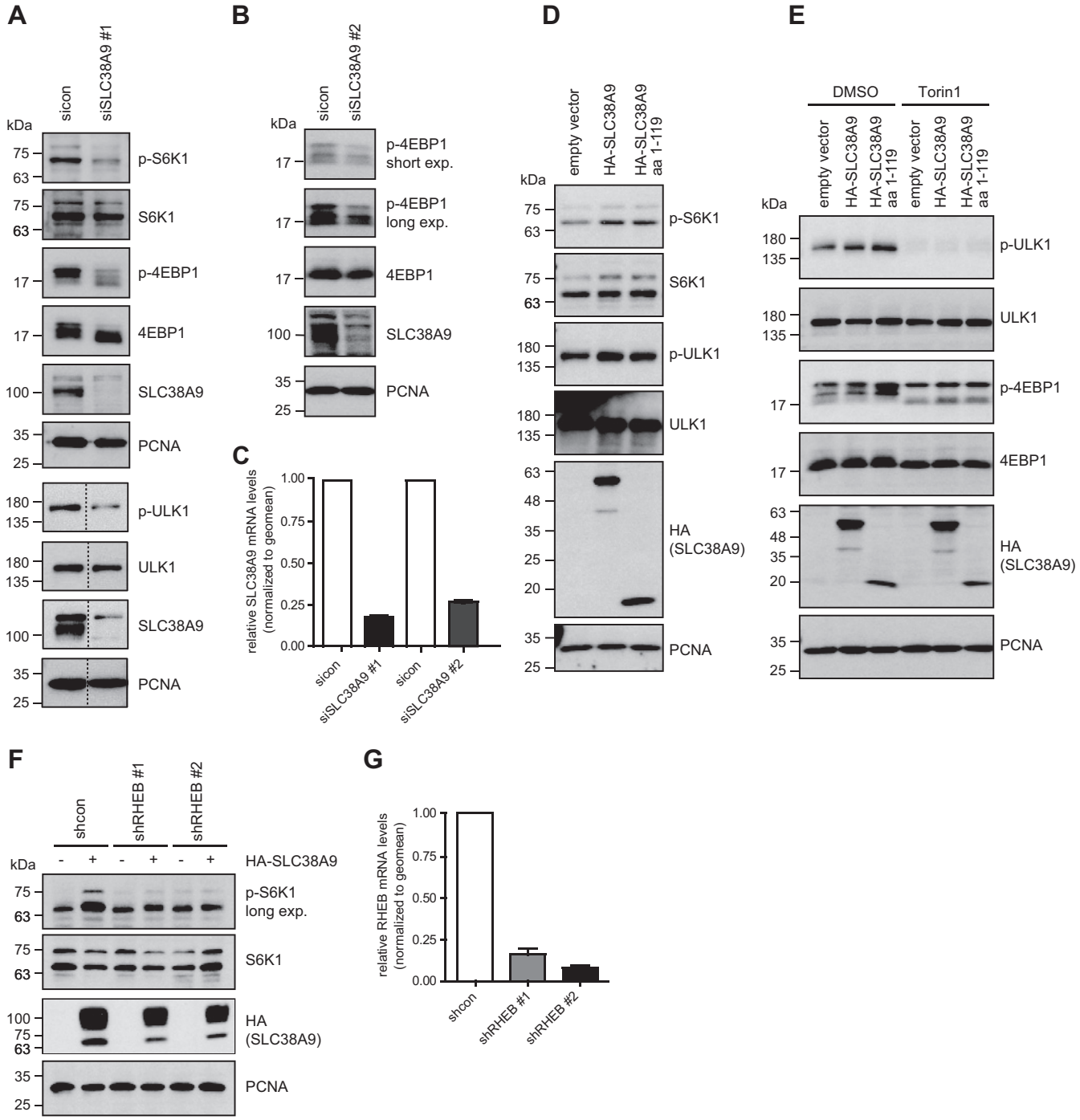

FIG 7 SLC38A9 regulates mTORC1 activity. (A and B) 293T cells were transfected with different nontargeting control (sicon) or *SLC38A9* siRNAs as indicated. Cell lysates were subjected to SDS-PAGE and immunoblotting. The phosphorylation status of S6K (A), ULK1 (A), and 4EBP1 (A and B) was determined using phospho-specific antibodies. PCNA served as a loading control. exp., exposure. (C) SLC38A9 knockdown in panels A and B additionally was confirmed by RT-qPCR. geomean, geometrical means. (D) 293T cells were transfected with HA-SLC38A9 full length, HA-SLC38A9 aa 1 to 119, or empty vector. Forty-eight hours posttransfection, cells were lysed and the phosphorylation status of mTORC1 substrates was determined using phospho-specific antibodies. PCNA served as a loading control. (E) Cells transfected as described for panel D were treated with Torin1 (1 h, 250 nM) or dimethyl sulfoxide (DMSO) as a control and analyzed as described for panel D. (F) Stable shRNA-mediated RHEB GTPase depletion or control 293T cells were transfected with HA-SLC38A9 full length or empty vector, respectively, followed by SDS-PAGE and immunoblotting. mTORC1 activity was assessed by determining the phosphorylation status of S6K. (G) RHEB GTPase knockdown shown in panel F was confirmed by RT-qPCR.

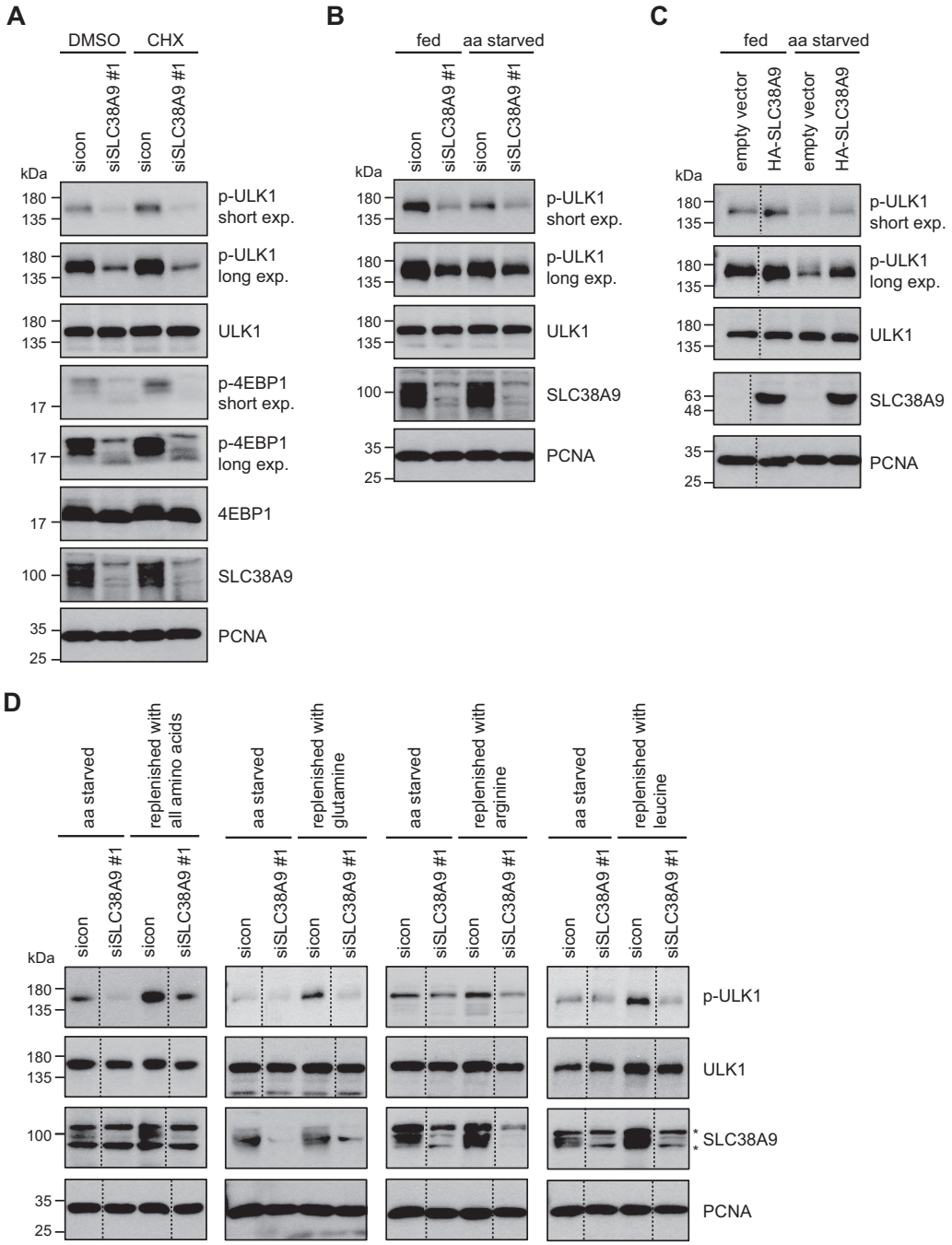

FIG 8 SLC38A9 regulates mTORC1 activity upon amino acid availability. (A and B) Seventy-two hours after transfection with nontargeting control (sicon) or *SLC38A9* siRNA, 293T cells were treated with CHX (2 h, 2 μg/ml) or DMSO as a control (A) or were fed or amino acid starved for 50 min (B), as indicated. Cell lysates were subjected to SDS-PAGE and immunoblotting with the indicated antibodies. PCNA served as the loading control. (C) Lysates from 293T cells transfected with HA-SLC38A9 or empty vector were fed or amino acid starved for 50 min and analyzed by immunoblotting with the indicated antibodies. PCNA served as a loading control. (D) 293T cells transfected with nontargeting control (sicon) or *SLC38A9* siRNA were either subjected to amino acid starvation for 50 min or amino acid starved for 50 min and then replenished for 10 min with the indicated amino acids. The phosphorylation status of ULK1 was determined using a phospho-specific antibody. PCNA served as the loading control. An asterisk indicates a nonspecific band.

SLC38A9 was required to retain amino acid-sensitive association with Rag proteins. Endogenous SLC38A9 colocalized with lysosomes and Rag-Ragulator complex components. Overexpression and depletion of SLC38A9 stimulated and inhibited mTORC1 activity, respectively, under fed conditions, while knockdown of SLC38A9 rendered cells effectively insensitive to changes in amino acid availability. Intriguingly, in the absence of SLC38A9, mTOR failed to translocate from the lysosome to the cytosol in response to amino acid starvation. Thus, our data confirm the two initial studies of Rebsamen et al. and Wang et al. (25, 26), collectively

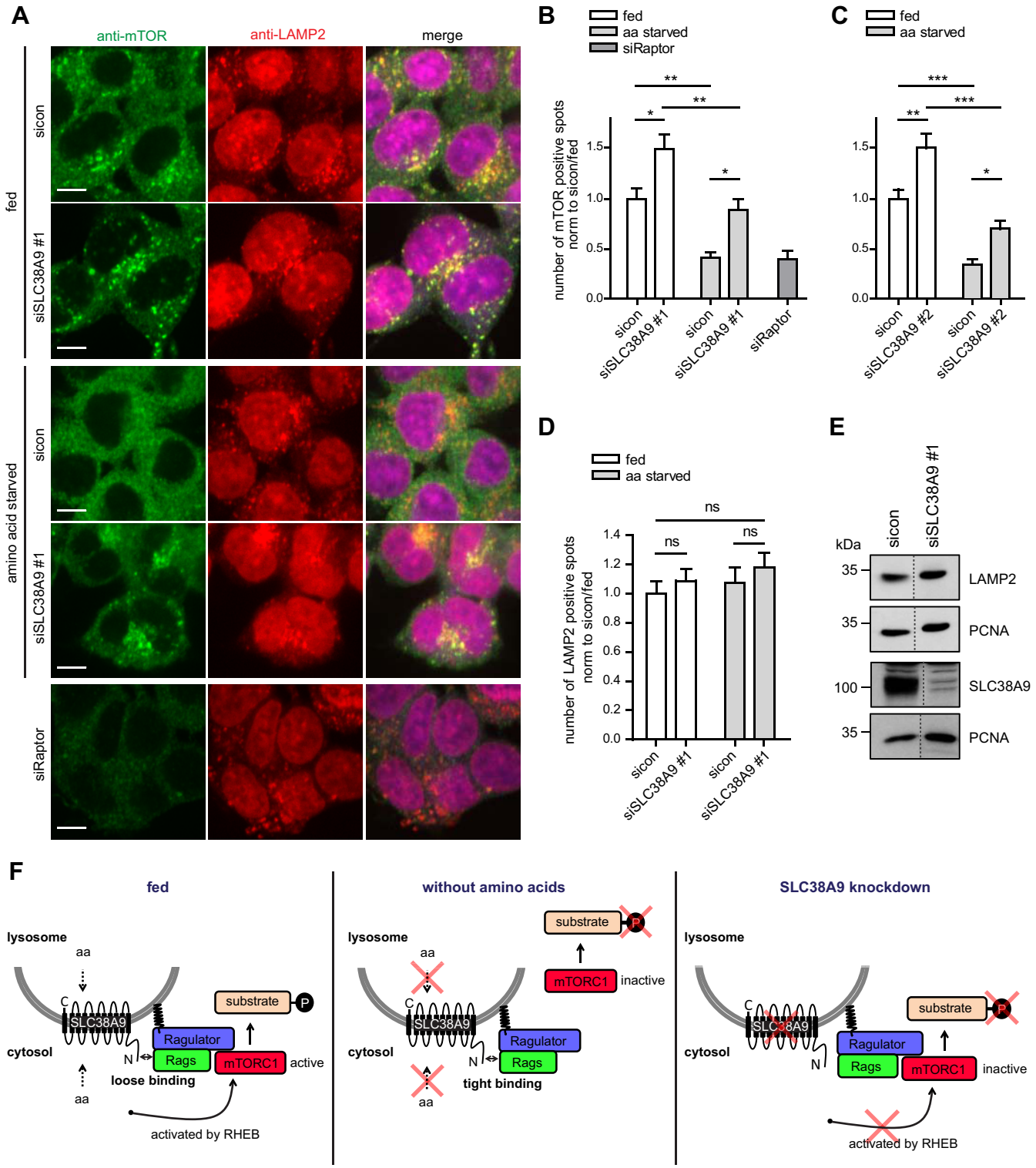

FIG 9 SLC38A9 depletion affects mTOR relocation from lysosomes to the cytosol. (A to D) 293T cells transfected with nontargeting control (sicon) or *SLC38A9* siRNA were fixed and labeled with anti-mTOR and anti-LAMP2 antibodies. Scale bar, 10 μm. (A) Example images. Quantification of mTOR (B and C)- and LAMP2 (D)-positive spots for a total of at least 40,000 ($n = 4$) (B), 110,000 ($n = 5$) (C), or 19,000 ($n = 3$) (D) cells was performed. norm to sicon/fed, normalized to sicon under fed conditions. Data represent means ± SEM, and statistical analysis was performed using GraphPad Prism. Statistical significance was determined with two-way ANOVA followed by Bonferroni's *post hoc* test (*, $P < 0.05$; **, $P < 0.01$; ***, $P < 0.001$). (E) 293T cells were transfected with nontargeting control (sicon) or *SLC38A9* siRNA. Seventy-two hours posttransfection, cells were lysed and LAMP2 protein levels were analyzed by SDS-PAGE and immunoblotting. PCNA served as a loading control. (F) SLC38A9 interacts with the Rag-Ragulator complex via its N-terminal cytosolic domain depending on the cellular amino acid status, thereby regulating amino acid-dependent mTOR localization and mTORC1 activity.

demonstrating that SLC38A9 functions as a lysosomal amino acid transporter and regulates mTORC1 activity via the Rag-Ragulator complex.

Several amino acid transporters of the SLC protein family have been implicated in mTORC1 regulation. For example, SLC1A5 and SLC3A2 control mTORC1 activity specifically upon glutamine transport (38), while inhibition of amino acid transport through SLC38A2 activates mTORC1 (40). However, the plasma membrane localization of SLC1A5, SLC3A2, and SLC38A2 makes them ineligible for sensing amino acids at lysosomes. In contrast, SLC36A1, an amino acid and proton symporter, localizes to the plasma membrane and intracellular membranes, such as the lysosome (41, 42). Since SLC36A1 was reported to interact with Rag GTPases (43) and to be required for mTOR recruitment to the lysosomal surface (43), SLC36A1 has been suggested to regulate mTORC1 activity as an amino acid transceptor. However, the fact that the amino acid preferences of the SLC36 protein family for alanine and proline do not match those amino acids that are involved in regulating mTORC1 activity (38, 41, 44) argues against a role of SLC36A1 as a lysosomal amino acid sensor for mTORC1. Several members of the SLC38 family have been shown to transport glutamine (45–52), which, together with arginine and leucine, stimulates mTORC1 activity (15, 38, 39). As established recently, SLC38A9 transports amino acids, although with conflicting amino acid preferences. Whereas Rebsamen et al. showed transport activity of SLC38A9 for glutamine (25), Wang et al. demonstrated arginine transport (26), while leucine could compete for the transport of both amino acids (25, 26). Consistent with these findings, our study revealed that replenishment with leucine, arginine, or glutamine following amino acid starvation failed to activate mTORC1 in the absence of SLC38A9, suggesting that SLC38A9 is required for the signaling availability of several different amino acids to mTORC1. Concurrent with a function as an amino acid transporter (25, 26) at the lysosome, only SLC38A9 encompassing the transmembrane domain associated with Rag proteins in an amino acid-sensitive manner, whereas the N-terminal, cytosolic fragment of SLC38A9 lacked this feature. Thus, several lines of evidence indicate that SLC38A9 is a transmembrane protein implicated in amino acid-dependent regulation of mTORC1.

Exactly how SLC38A9 signals amino acid availability to the Rag-Ragulator complex currently is not clear. Our observation that association between SLC38A9 and Rag GTPases is amino acid sensitive suggests that the domains mediating this interaction undergo conformational changes in response to amino acid availability. The amino acid-transporting transmembrane domain of SLC38A9 would be an obvious candidate for inducing a switch between different conformational states. In support of this hypothesis, overexpression of the cytosolic domain of SLC38A9 alone was sufficient to stimulate mTORC1 activity. Moreover, binding of the cytosolic domain of SLC38A9 to Rag GTPases was independent of amino acids. Thus, uncoupled from its transmembrane domain, the cytosolic domain of SLC38A9 might be locked in the activating conformation.

Cycling of mTOR between cytosol and lysosome generally is coupled to its inactive and active states, respectively, and depends on Rag GTPases, Ragulator, TSC, and RHEB GTPase (9, 16, 23, 31). Surprisingly, depletion of SLC38A9 retained inactive mTORC1 at the lysosome under amino acid-fed and -starved conditions, indicating that signaling amino acid depletion through SLC38A9 is required for releasing Rag-Ragulator-bound mTORC1 from lysosomal membranes. A possible scenario is that differential binding of SLC38A9 to Rag and/or LAMTOR proteins primes Rag-Ragulator-bound mTORC1 for activation by inducing structural rearrangements in this complex. While the composition of all three complexes did not change in the absence of SLC38A9, it remains possible that conformational changes within and altered binding affinities among the complexes result in the retention of inactive mTORC1 at the lysosome. A second possibility is that SLC38A9 contributes to recruitment or spatial organization of RHEB to mTORC1 given that SLC38A9 overexpression-induced hyperactivation of mTORC1 was decreased upon RHEB GTPase depletion. Since lysosomal recruitment of TSC2 by the Rag GTPases is necessary to release mTORC1 to the cytoplasm upon amino acid starvation dependent on RHEB GTPase (31), we further hypothesize that SLC38A9 depletion affects the RHEB GAP TSC. Alternatively, as SLC38A9 preferentially binds to the Rag mutant heterodimer in which RRAGB and RRAGC are GDP and GTP locked, respectively, SLC38A9 could also regulate the GEF activity of the Ragulator complex, thereby stimulating mTOR release to the cytoplasm. In support of this hypothesis, we found that overexpressed myc-tagged LAMTOR2 increasingly binds to Rag GTPase heterodimers when SLC38A9 is depleted. Thus, loss of SLC38A9 could lead to hyperactivated GEF activity of the Ragulator complex and retention of mTOR on the lysosomal membrane. Clearly, further studies are needed to evaluate these hypotheses and to fully decipher how SLC38A9 contributes mechanistically to amino acid sensing and signaling to mTORC1.

mTORC1 activity depends on the intracellular position of lysosomes, which in turn is dependent on the intracellular pH (33, 53). Perinuclear positioning of lysosomes retain inactive mTORC1 using mild starvation conditions, while nutrient replenishment causes the redistribution of lysosomes to the cellular periphery accompanied by increased mTORC1 activity (33). Upon SLC38A9 depletion, lysosomes seem to cluster more in the perinuclear region, which would be consistent with mTORC1 inactivity. As SLC38A9 amino acid transport is pH dependent (25), it also might be involved in the proper distribution of lysosomes by sensing intracellular pH or by influencing transport proteins, given that we found many trafficking proteins associated with SLC38A9.

Based on the current findings, we propose the following working model for SLC38A9. Under fed conditions, SLC38A9 transports amino acids and signals their presence via association of its cytosolic domain with the Rag-Ragulator complex. This in turn recruits mTOR to the lysosomal surface, where it is activated by RHEB. Under starvation conditions, the interaction between SLC38A9 and the Rag GTPases is tightened, possibly by a conformational change within the cytosolic domain of SLC38A9 induced by the absence of amino acids sensed by the transmembrane domain region of SLC38A9. The altered interaction between SLC38A9 and Rag proteins in the absence of amino acids may induce the release of mTORC1 to the cytoplasm via an unknown mechanism where mTORC1 resides in an inactive state. In the absence of SLC38A9, mTOR translocates to the lysosome but can neither be efficiently activated under fed conditions nor be released to the cytosol in its inactive form when cells undergo amino acid starvation (Fig. 9F).

Thus, our work adds to the compelling evidence that reveals SLC38A9 as a lysosomal amino acid transporter regulating mTORC1 activity. Given that mTORC1 kinase activity is deregu-

lated in many cancers (1) and that 60% of approved drug targets are membrane proteins (54), SLC38A9 may serve as a new target to control mTORC1 activity.

ACKNOWLEDGMENTS

We are grateful to J. W. Harper for critical access to CompPASS. We thank S. Müller, I. Dikic, and S. Oess for readily sharing protocols and reagents and D. McEwan for helpful discussions. Anti-Deptor antibody and RHEB GTPase cDNA were kind gifts from I. Dikic. We received RHEB shRNAs from S. Fulda. We are thankful to members of the Behrends laboratory for resources and discussions. We thank I. Dikic for generous support.

This work was supported by grants from the German Research Foundation (BE 4685/1-1) and the European Research Council (282333).

J.J. and H.M.G. performed all experiments. C.B. and J.J. conceived the study. J.J., H.M.G., and C.B. wrote the manuscript.

REFERENCES

1. **Guertin DA, Sabatini DM.** 2007. Defining the role of mTOR in cancer. Cancer Cell **12:**9–22. http://dx.doi.org/10.1016/j.ccr.2007.05.008.
2. **Kim DH, Sarbassov DD, Ali SM, King JE, Latek RR, Erdjument-Bromage H, Tempst P, Sabatini DM.** 2002. mTOR interacts with raptor to form a nutrient-sensitive complex that signals to the cell growth machinery. Cell **110:**163–175. http://dx.doi.org/10.1016/S0092-8674(02)00808-5.
3. **Kim DH, Sarbassov DD, Ali SM, Latek RR, Guntur KV, Erdjument-Bromage H, Tempst P, Sabatini DM.** 2003. GbetaL, a positive regulator of the rapamycin-sensitive pathway required for the nutrient-sensitive interaction between raptor and mTOR. Mol Cell **11:**895–904. http://dx.doi.org/10.1016/S1097-2765(03)00114-X.
4. **Sengupta S, Peterson TR, Sabatini DM.** 2010. Regulation of the mTOR complex 1 pathway by nutrients, growth factors, and stress. Mol Cell **40:**310–322. http://dx.doi.org/10.1016/j.molcel.2010.09.026.
5. **Dibble CC, Elis W, Menon S, Qin W, Klekota J, Asara JM, Finan PM, Kwiatkowski DJ, Murphy LO, Manning BD.** 2012. TBC1D7 is a third subunit of the TSC1-TSC2 complex upstream of mTORC1. Mol Cell **47:**535–546. http://dx.doi.org/10.1016/j.molcel.2012.06.009.
6. **Inoki K, Li Y, Xu T, Guan KL.** 2003. Rheb GTPase is a direct target of TSC2 GAP activity and regulates mTOR signaling. Genes Dev **17:**1829–1834. http://dx.doi.org/10.1101/gad.1110003.
7. **Tee AR, Manning BD, Roux PP, Cantley LC, Blenis J.** 2003. Tuberous sclerosis complex gene products, Tuberin and Hamartin, control mTOR signaling by acting as a GTPase-activating protein complex toward Rheb. Curr Biol **13:**1259–1268. http://dx.doi.org/10.1016/S0960-9822(03)00506-2.
8. **Groenewoud MJ, Zwartkruis FJ.** 2013. Rheb and Rags come together at the lysosome to activate mTORC1. Biochem Soc Trans **41:**951–955. http://dx.doi.org/10.1042/BST20130037.
9. **Sancak Y, Peterson TR, Shaul YD, Lindquist RA, Thoreen CC, Bar-Peled L, Sabatini DM.** 2008. The Rag GTPases bind raptor and mediate amino acid signaling to mTORC1. Science **320:**1496–1501. http://dx.doi.org/10.1126/science.1157535.
10. **Saito K, Araki Y, Kontani K, Nishina H, Katada T.** 2005. Novel role of the small GTPase Rheb: its implication in endocytic pathway independent of the activation of mammalian target of rapamycin. J Biochem **137:**423–430. http://dx.doi.org/10.1093/jb/mvi046.
11. **Buerger C, DeVries B, Stambolic V.** 2006. Localization of Rheb to the endomembrane is critical for its signaling function. Biochem Biophys Res Commun **344:**869–880. http://dx.doi.org/10.1016/j.bbrc.2006.03.220.
12. **Castro AF, Rebhun JF, Clark GJ, Quilliam LA.** 2003. Rheb binds tuberous sclerosis complex 2 (TSC2) and promotes S6 kinase activation in a rapamycin- and farnesylation-dependent manner. J Biol Chem **278:**32493–32496. http://dx.doi.org/10.1074/jbc.C300226200.
13. **Long X, Lin Y, Ortiz-Vega S, Yonezawa K, Avruch J.** 2005. Rheb binds and regulates the mTOR kinase. Curr Biol **15:**702–713. http://dx.doi.org/10.1016/j.cub.2005.02.053.
14. **Yadav RB, Burgos P, Parker AW, Iadevaia V, Proud CG, Allen RA, O'Connell JP, Jeshtadi A, Stubbs CD, Botchway SW.** 2013. mTOR direct interactions with Rheb-GTPase and raptor: sub-cellular localization using fluorescence lifetime imaging. BMC Cell Biol **14:**3. http://dx.doi.org/10.1186/1471-2121-14-3.
15. **Hara K, Yonezawa K, Weng QP, Kozlowski MT, Belham C, Avruch J.** 1998. Amino acid sufficiency and mTOR regulate p70 S6 kinase and eIF-4E BP1 through a common effector mechanism. J Biol Chem **273:**14484–14494. http://dx.doi.org/10.1074/jbc.273.23.14484.
16. **Sancak Y, Bar-Peled L, Zoncu R, Markhard AL, Nada S, Sabatini DM.** 2010. Ragulator-Rag complex targets mTORC1 to the lysosomal surface and is necessary for its activation by amino acids. Cell **141:**290–303. http://dx.doi.org/10.1016/j.cell.2010.02.024.
17. **Kim MS, Kuehn HS, Metcalfe DD, Gilfillan AM.** 2008. Activation and function of the mTORC1 pathway in mast cells. J Immunol **180:**4586–4595. http://dx.doi.org/10.4049/jimmunol.180.7.4586.
18. **Sekiguchi T, Hirose E, Nakashima N, Ii M, Nishimoto T.** 2001. Novel G proteins, Rag C and Rag D, interact with GTP-binding proteins, Rag A and Rag B. J Biol Chem **276:**7246–7257. http://dx.doi.org/10.1074/jbc.M004389200.
19. **Schurmann A, Brauers A, Massmann S, Becker W, Joost HG.** 1995. Cloning of a novel family of mammalian GTP-binding proteins (RagA, RagBs, RagB1) with remote similarity to the Ras-related GTPases. J Biol Chem **270:**28982–28988. http://dx.doi.org/10.1074/jbc.270.48.28982.
20. **Tsun ZY, Bar-Peled L, Chantranupong L, Zoncu R, Wang T, Kim C, Spooner E, Sabatini DM.** 2013. The folliculin tumor suppressor is a GAP for the RagC/D GTPases that signal amino acid levels to mTORC1. Mol Cell **52:**495–505. http://dx.doi.org/10.1016/j.molcel.2013.09.016.
21. **Bar-Peled L, Chantranupong L, Cherniack AD, Chen WW, Ottina KA, Grabiner BC, Spear ED, Carter SL, Meyerson M, Sabatini DM.** 2013. A tumor suppressor complex with GAP activity for the Rag GTPases that signal amino acid sufficiency to mTORC1. Science **340:**1100–1106. http://dx.doi.org/10.1126/science.1232044.
22. **Han JM, Jeong SJ, Park MC, Kim G, Kwon NH, Kim HK, Ha SH, Ryu SH, Kim S.** 2012. Leucyl-tRNA synthetase is an intracellular leucine sensor for the mTORC1-signaling pathway. Cell **149:**410–424. http://dx.doi.org/10.1016/j.cell.2012.02.044.
23. **Bar-Peled L, Schweitzer LD, Zoncu R, Sabatini DM.** 2012. Ragulator is a GEF for the rag GTPases that signal amino acid levels to mTORC1. Cell **150:**1196–1208. http://dx.doi.org/10.1016/j.cell.2012.07.032.
24. **Zoncu R, Bar-Peled L, Efeyan A, Wang S, Sancak Y, Sabatini DM.** 2011. mTORC1 senses lysosomal amino acids through an inside-out mechanism that requires the vacuolar H(+)-ATPase. Science **334:**678–683. http://dx.doi.org/10.1126/science.1207056.
25. **Rebsamen M, Pochini L, Stasyk T, de Araujo ME, Galluccio M, Kandasamy RK, Snijder B, Fauster A, Rudashevskaya EL, Bruckner M, Scorzoni S, Filipek PA, Huber KV, Bigenzahn JW, Heinz LX, Kraft C, Bennett KL, Indiveri C, Huber LA, Superti-Furga G.** 2015. SLC38A9 is a component of the lysosomal amino acid sensing machinery that controls mTORC1. Nature **519:**477–481. http://dx.doi.org/10.1038/nature14107.
26. **Wang S, Tsun ZY, Wolfson RL, Shen K, Wyant GA, Plovanich ME, Yuan ED, Jones TD, Chantranupong L, Comb W, Wang T, Bar-Peled L, Zoncu R, Straub C, Kim C, Park J, Sabatini BL, Sabatini DM.** 2015. Metabolism. Lysosomal amino acid transporter SLC38A9 signals arginine sufficiency to mTORC1. Science **347:**188–194. http://dx.doi.org/10.1126/science.1257132.
27. **Behrends C, Sowa ME, Gygi SP, Harper JW.** 2010. Network organization of the human autophagy system. Nature **466:**68–76. http://dx.doi.org/10.1038/nature09204.
28. **Sowa ME, Bennett EJ, Gygi SP, Harper JW.** 2009. Defining the human deubiquitinating enzyme interaction landscape. Cell **138:**389–403. http://dx.doi.org/10.1016/j.cell.2009.04.042.
29. **Huttlin EL, Jedrychowski MP, Elias JE, Goswami T, Rad R, Beausoleil SA, Villen J, Haas W, Sowa ME, Gygi SP.** 2010. A tissue-specific atlas of mouse protein phosphorylation and expression. Cell **143:**1174–1189. http://dx.doi.org/10.1016/j.cell.2010.12.001.
30. **Smith EM, Finn SG, Tee AR, Browne GJ, Proud CG.** 2005. The tuberous sclerosis protein TSC2 is not required for the regulation of the mammalian target of rapamycin by amino acids and certain cellular stresses. J Biol Chem **280:**18717–18727. http://dx.doi.org/10.1074/jbc.M414499200.
31. **Demetriades C, Doumpas N, Teleman AA.** 2014. Regulation of TORC1 in response to amino acid starvation via lysosomal recruitment of TSC2. Cell **156:**786–799. http://dx.doi.org/10.1016/j.cell.2014.01.024.
32. **Krogh A, Larsson B, von Heijne G, Sonnhammer EL.** 2001. Predicting transmembrane protein topology with a hidden Markov model: application to complete genomes. J Mol Biol **305:**567–580. http://dx.doi.org/10.1006/jmbi.2000.4315.
33. **Korolchuk VI, Saiki S, Lichtenberg M, Siddiqi FH, Roberts EA, Imarisio**

S, Jahreiss L, Sarkar S, Futter M, Menzies FM, O'Kane CJ, Deretic V, Rubinsztein DC. 2011. Lysosomal positioning coordinates cellular nutrient responses. Nat Cell Biol **13:**453–460. http://dx.doi.org/10.1038/ncb2204.

34. **Schioth HB, Roshanbin S, Hagglund MG, Fredriksson R.** 2013. Evolutionary origin of amino acid transporter families SLC32, SLC36 and SLC38 and physiological, pathological and therapeutic aspects. Mol Aspects Med **34:**571–585. http://dx.doi.org/10.1016/j.mam.2012.07.012.
35. **Fletcher JS, Beevers H.** 1971. Influence of cycloheximide on the synthesis and utilization of amino acids in suspension cultures. Plant Physiol **48:**261–264. http://dx.doi.org/10.1104/pp.48.3.261.
36. **Widuczynski I, Stoppani AO.** 1965. Action of cycloheximide on amino acid metabolism in Saccharomyces elipsoideus. Biochim Biophys Acta **104:**413–426. http://dx.doi.org/10.1016/0304-4165(65)90347-8.
37. **Beugnet A, Tee AR, Taylor PM, Proud CG.** 2003. Regulation of targets of mTOR (mammalian target of rapamycin) signalling by intracellular amino acid availability. Biochem J **372:**555–566. http://dx.doi.org/10.1042/BJ20021266.
38. **Nicklin P, Bergman P, Zhang B, Triantafellow E, Wang H, Nyfeler B, Yang H, Hild M, Kung C, Wilson C, Myer VE, MacKeigan JP, Porter JA, Wang YK, Cantley LC, Finan PM, Murphy LO.** 2009. Bidirectional transport of amino acids regulates mTOR and autophagy. Cell **136:**521–534. http://dx.doi.org/10.1016/j.cell.2008.11.044.
39. **Wang X, Campbell LE, Miller CM, Proud CG.** 1998. Amino acid availability regulates p70 S6 kinase and multiple translation factors. Biochem J **334**(Part 1)**:**261–267.
40. **Pinilla J, Aledo JC, Cwiklinski E, Hyde R, Taylor PM, Hundal HS.** 2011. SNAT2 transceptor signalling via mTOR: a role in cell growth and proliferation? Front Biosci **3:**1289–1299. http://dx.doi.org/10.2741/332.
41. **Sagne C, Agulhon C, Ravassard P, Darmon M, Hamon M, El Mestikawy S, Gasnier B, Giros B.** 2001. Identification and characterization of a lysosomal transporter for small neutral amino acids. Proc Natl Acad Sci U S A **98:**7206–7211. http://dx.doi.org/10.1073/pnas.121183498.
42. **Agulhon C, Rostaing P, Ravassard P, Sagne C, Triller A, Giros B.** 2003. Lysosomal amino acid transporter LYAAT-1 in the rat central nervous system: an in situ hybridization and immunohistochemical study. J Comp Neurol **462:**71–89. http://dx.doi.org/10.1002/cne.10712.
43. **Ogmundsdottir MH, Heublein S, Kazi S, Reynolds B, Visvalingam SM, Shaw MK, Goberdhan DC.** 2012. Proton-assisted amino acid transporter PAT1 complexes with Rag GTPases and activates TORC1 on late endosomal and lysosomal membranes. PLoS One **7:**e36616. http://dx.doi.org/10.1371/journal.pone.0036616.
44. **Edwards N, Anderson CM, Gatfield KM, Jevons MP, Ganapathy V, Thwaites DT.** 2011. Amino acid derivatives are substrates or non-transported inhibitors of the amino acid transporter PAT2 (slc36a2). Biochim Biophys Acta **1808:**260–270. http://dx.doi.org/10.1016/j.bbamem.2010.07.032.
45. **Sugawara M, Nakanishi T, Fei YJ, Huang W, Ganapathy ME, Leibach FH, Ganapathy V.** 2000. Cloning of an amino acid transporter with functional characteristics and tissue expression pattern identical to that of system A. J Biol Chem **275:**16473–16477. http://dx.doi.org/10.1074/jbc.C000205200.
46. **Yao D, Mackenzie B, Ming H, Varoqui H, Zhu H, Hediger MA, Erickson JD.** 2000. A novel system A isoform mediating Na+/neutral amino acid cotransport. J Biol Chem **275:**22790–22797. http://dx.doi.org/10.1074/jbc.M002965200.
47. **Hatanaka T, Huang W, Ling R, Prasad PD, Sugawara M, Leibach FH, Ganapathy V.** 2001. Evidence for the transport of neutral as well as cationic amino acids by ATA3, a novel and liver-specific subtype of amino acid transport system A. Biochim Biophys Acta **1510:**10–17. http://dx.doi.org/10.1016/S0005-2736(00)00390-4.
48. **Sugawara M, Nakanishi T, Fei YJ, Martindale RG, Ganapathy ME, Leibach FH, Ganapathy V.** 2000. Structure and function of ATA3, a new subtype of amino acid transport system A, primarily expressed in the liver and skeletal muscle. Biochim Biophys Acta **1509:**7–13. http://dx.doi.org/10.1016/S0005-2736(00)00349-7.
49. **Chaudhry FA, Reimer RJ, Krizaj D, Barber D, Storm-Mathisen J, Copenhagen DR, Edwards RH.** 1999. Molecular analysis of system N suggests novel physiological roles in nitrogen metabolism and synaptic transmission. Cell **99:**769–780. http://dx.doi.org/10.1016/S0092-8674(00)81674-8.
50. **Nakanishi T, Kekuda R, Fei YJ, Hatanaka T, Sugawara M, Martindale RG, Leibach FH, Prasad PD, Ganapathy V.** 2001. Cloning and functional characterization of a new subtype of the amino acid transport system. N Am J Physiol Cell Physiol **281:**C1757–C1768.
51. **Varoqui H, Zhu H, Yao D, Ming H, Erickson JD.** 2000. Cloning and functional identification of a neuronal glutamine transporter. J Biol Chem **275:**4049–4054. http://dx.doi.org/10.1074/jbc.275.6.4049.
52. **Hagglund MG, Sreedharan S, Nilsson VC, Shaik JH, Almkvist IM, Backlin S, Wrange O, Fredriksson R.** 2011. Identification of SLC38A7 (SNAT7) protein as a glutamine transporter expressed in neurons. J Biol Chem **286:**20500–20511. http://dx.doi.org/10.1074/jbc.M110.162404.
53. **Heuser J.** 1989. Changes in lysosome shape and distribution correlated with changes in cytoplasmic pH. J Cell Biol **108:**855–864. http://dx.doi.org/10.1083/jcb.108.3.855.
54. **Yildirim MA, Goh KI, Cusick ME, Barabasi AL, Vidal M.** 2007. Drug-target network. Nat Biotechnol **25:**1119–1126. http://dx.doi.org/10.1038/nbt1338.